



Cooperative Research Centre for
Landscape Environments
and Mineral Exploration



OPEN FILE
REPORT
SERIES

GOLD DISPERSION IN THE REGOLITH AT THE FEDERAL DEPOSIT, WESTERN AUSTRALIA.

N.B. Sergeev and D.J. Gray

CRC LEME OPEN FILE REPORT 223

November 2008

CRCLEME

(CRC LEME Restricted Report I32R / E&M Report 704R, 2000
2nd Impression 2008)

CRC LEME is an unincorporated joint venture between CSIRO-Exploration & Mining, and Land & Water, The Australian National University, Curtin University of Technology, University of Adelaide, Geoscience Australia, Primary Industries and Resources SA, NSW Department of Primary Industries and Minerals Council of Australia, established and supported under the Australian Government's Cooperative Research Centres Program.





GOLD DISPERSION IN THE REGOLITH AT THE FEDERAL DEPOSIT, WESTERN AUSTRALIA.

N.B. Sergeev and D.J. Gray

CRC LEME OPEN FILE REPORT 223

November 2008

(CRC LEME Restricted Report 132R / E&M Report 704R, 2000
2nd Impression 2008)

© CRC LEME 2000

CRC LEME is an unincorporated joint venture between CSIRO-Exploration & Mining, and Land & Water, The Australian National University, Curtin University of Technology, University of Adelaide, Geoscience Australia, Primary Industries and Resources SA, NSW Department of Primary Industries and Minerals Council of Australia.

Headquarters: CRC LEME c/o CSIRO Exploration and Mining, PO Box 1130, Bentley WA 6102, Australia

The CRC LEME–AMIRA Project 504 “**SUPERGENE MOBILIZATION OF GOLD IN THE YILGARN CRATON**” was carried out over the period 1998 to 2001. Twelve reports resulted from this collaborative project.

CRC LEME acknowledges the support of companies associated with and represented by the Australian Mineral Industries Research Association (AMIRA), and the major contribution of researchers from CSIRO Exploration and Mining.

Although the confidentiality periods of the research reports have expired, the last in July 2002, they have not been made public until now. In line with CRC LEME technology transfer goals, re-releasing the reports through the **CRC LEME Open File Report (OFR) Series** is seen as an appropriate means of making available to the mineral exploration industry, the results of the research and the authors’ interpretations. It is hoped that the reports will provide a source for reference and be useful for teaching.

OFR 217 – Characteristics of gold distribution and hydrogeochemistry at the Carosue Dam prospect, Western Australia – DJ Gray, NB Sergeev and CG Porto.

OFR 218 – Gold distribution, regolith and groundwater characteristics at the Mt Joel prospect, Western Australia – CG Porto, NB Sergeev and DJ Gray.

OFR 219 – Supergene gold dispersion at the Argo and Apollo deposits, Western Australia – AF Britt and DJ Gray

OFR 220 – Geochemistry, hydrogeochemistry and mineralogy of regolith, Twin peaks and Monty Dam gold prospects, Western Australia – NB Sergeev and DJ Gray.

OFR 221 - Supergene gold dispersion in the Panglo Gold deposit, Western Australia – DJ Gray.

OFR 222 – Gold concentration in the regolith at the Mt Joel prospect, Western Australia – DJ Gray.

OFR 223 – Gold dispersion in the regolith at the Federal Deposit, Western Australia – NB Sergeev and DJ Gray.

OFR 224 – Supergene gold dispersion in the regolith at the Cleo deposit, Western Australia – AF Britt and DJ Gray.

OFR 225 – Distribution of gold arsenic chromium and copper in the regolith at the Harmony Deposit, northern Yilgarn, Western Australia – AF Britt and DJ Gray

OFR 226 – Supergene gold dispersion in the regolith at the Kanowna Belle and Ballarat Last Chance deposits, Western Australia – DJ Gray

OFR 227 – Supergene gold dispersion, regolith and groundwater of the Mt Holland region, Southern Cross province, Western Australia – AF Britt and DJ Gray.

OFR 228 – Supergene mobilization of gold and other elements in the Yilgarn Craton, *Western Australia* – **FINAL REPORT** – DJ Gray, NB Sergeev, CG Porto and AF Britt

This Open File Report 223 is a second impression (updated second printing) of CRC for Landscape Evolution and Mineral Exploration Restricted Report No 132R, first issued in May 2000. It has been re-printed by CRC for Landscape Environments and Mineral Exploration (CRC LEME).

Electronic copies of the publication in PDF format can be downloaded from the CRC LEME website: <http://crlceme.org.au/Pubs/OFRSindex.html>. Information on this or other LEME publications can be obtained from <http://crlceme.org.au>.

Hard copies will be retained in the Australian National Library, the J. S. Battye Library of West Australian History, and the CSIRO Library at the Australian Resources Research Centre, Kensington, Western Australia.

Reference:

Sergeev, N.B. and Gray, D.J. 2000. Gold dispersion in the regolith at the Federal Deposit, Western Australia. CRC LEME Restricted Report 132R, 152 pp. (Reissued as Open File Report 223, CRC LEME, Perth, 2008). Also originally recorded as CSIRO Exploration and Mining Restricted Report 704R, 2000.

Keywords: 1. Supergene gold 2. Mobilization of gold 3. Geochemistry 4. Hydrogeochemistry 5. Federal Gold Prospect - Western Australia 6. Regolith 7. 3-D Modeling 8. Gold Grain Analysis

ISSN 1329-4768

ISBN 1 921039 68X

Addresses and affiliations of Authors:

N.B. Sergeev¹ and D.J. Gray
CRC LEME
c/o CSIRO Exploration and Mining
PO Box 1130, Bentley,
Western Australia 6102.
(¹Previously)

Published by: CRC LEME
c/o CSIRO Exploration and Mining
PO Box 1130, Bentley, Western Australia 6102.

Disclaimer

The user accepts all risks and responsibility for losses, damages, costs and other consequences resulting directly or indirectly from using any information or material contained in this report. To the maximum permitted by law, CRC LEME excludes all liability to any person arising directly or indirectly from using any information or material contained in this report.

© **This report is Copyright** of the Cooperative Research Centre for Landscape Evolution and Mineral Exploration 2000, which resides with its Core Participants: CSIRO Exploration and Mining, University of Canberra, The Australian National University, Geoscience Australia (formerly Australian Geological Survey Organisation).

Apart from any fair dealing for the purposes of private study, research, criticism or review, as permitted under Copyright Act, no part may be reproduced or reused by any process whatsoever, without prior written approval from the Core Participants mentioned above.

PREFACE

The CRC LEME-AMIRA Project 504 *Supergene mobilization of gold and other elements in the Yilgarn Craton* has, as its principal objective, determination of the mechanisms of supergene/secondary depletion, enrichment and dispersion of Au and other elements, so as to improve selection of drilling targets and further optimize interpretation of geochemical data. For this goal, it is important to develop methods for recognition and understanding of any supergene mobilization of Au and potential pathfinder elements. This report summarizes investigations undertaken at Federal Au deposit and the surrounding Woodcutters exploration area by CRCLEME as part of Project 504.

The Federal deposit is located about 40 km NNW of Kalgoorlie and is one of few relatively large Au deposits in the Yilgarn Craton hosted by granitoids. The deposit is deeply weathered and overlain by transported overburden; it was discovered in 1996 using an adjacent calcrete Au anomaly. This report gives the results on the regolith stratigraphy, Au geochemistry and hydrogeochemistry in the Woodcutters area, focusing on characteristics of the supergene Au enrichments and dispersion haloes in the residuum and transported overburden. Supergene Au enrichments are well developed in the area, providing a valuable study site for enhancing the knowledge of supergene Au mobilization in different environments of the Yilgarn Craton.

D.J. Gray,
Project Leader.
May, 2000

ABSTRACT

The dispersion of Au in the regolith and groundwater has been studied at the Federal deposit, in the Woodcutters area, Western Australia. Gold mineralization occurs primarily as Au-quartz-pyrite veins, as well as Au and sulphide veinlets along a fracture system within granodiorites and monzogranites of the Scotia pluton.

In the Woodcutters area, granitoids of the Scotia pluton are deeply (up to 60 m) weathered, with a further deepening of 5-25 m over the Federal mineralized zone due to sulphide weathering. The granitoids are hornblende-rich, which has resulted in development of smectite in the saprolite. A continuous 2-16 m thick cover of transported overburden, consisting of duricrust and sandy colluvium, overlies the residual bleached clay saprolite. The regolith modification under semi-arid to arid conditions since the Miocene included silicification of the basal facies of the sediments and the top of the residual profile, hardpanization of the colluvium and development of pedogenic carbonates close to the surface.

At the Federal deposit, Au enrichment in the regolith occurs at two levels: near the weathering front and at the top of the transition zone. The lower enrichment zone is up to 27 m thick with Au maxima 6-12 m above the weathering front. Within the orebody, Au concentrations are 2-3-fold greater at this level, compared to the primary rock. The data indicate chemogenic Au redistribution from the upper regolith, given that the residual Au concentration in the saprolite is commonly less than 1.5 times that of the primary rock. The dispersion halo extends as a patchy cover to the east, up to approximately 400 m at a 60 ppb cut-off. The majority of the halo is located above the weakly mineralized (up to 30 ppb) primary rocks, suggesting that this blanket is due to a combination of residual and chemogenic Au accumulations.

The upper enrichment is several metres below the transition/oxide zone boundary. Within the orebody, supergene enrichment occurs as a chain of local Au-rich (up to 1 ppm) spots along the mineralized structure. The oxide zone above is Au depleted.

At the base of transported overburden, Au is concentrated in duricrust colluvium, mostly enclosed within ferruginous nodules and quartz, indicating mechanical transport of Au. Near the surface, in calcareous soil and colluvium, the majority of Au (83-97%) is enclosed within carbonate nodules indicating chemogenic Au mobilization in the calcrete environment. The morphology of supergene Au grains in carbonate nodules suggests a bacterial origin of the Au.

TABLE OF CONTENTS

1	INTRODUCTION	1
	1.1 Location.....	1
	1.2 Geology and mineralization.....	1
	1.3 Geomorphology, climate and vegetation	3
2	STUDY METHODS	4
	2.1 Sampling and analysis.....	4
	2.1.1 Drill hole and open pit sampling.....	4
	2.1.2 Chemical analysis	4
	2.1.3 Mineralogical analysis.....	4
	2.1.4 Gold grain separation and analysis	4
	2.1.5 Groundwater sampling and analysis	5
	2.2 3D gridding, visualization and Au concentration calculations	6
3	REGOLITH STRATIGRAPHY	8
	3.1 Comparison between Centaur and CRCLEME logging	8
	3.2 Centaur regolith stratigraphy.....	9
	3.3 CRCLEME regolith stratigraphy.....	11
	3.4 Transported overburden.....	14
	3.4.1 Transported overburden stratigraphy	14
	3.4.2 Discriminant analysis and geochemical characterization of transported overburden units.....	15
4	GOLD GEOCHEMISTRY	16
	4.1 Gold in residuum.....	16
	4.1.1 Patterns of gold distribution	16
	4.1.2 Gold concentration calculations	19
	4.1.3 Gold associations in residuum.....	21
	4.2 Gold in the transported overburden.....	22
	4.2.1 Gold distribution in the transported overburden.....	22
	4.2.2 Gold concentration calculations	23
	4.2.3 Gold mass balance in transported overburden.....	24
5	CHARACTERISTICS OF PARTICULATE GOLD AT FEDERAL.....	26
	5.1 Introduction.....	26
	5.2 Characteristics of gold grains	26
	5.2.1 Gold in primary mineralization	26
	5.2.2 Gold in the residual regolith.....	27
	5.2.3 Gold in carbonate materials	27
	5.3 Discussion.....	27
6	HYDROGEOCHEMISTRY	28
	6.1 Introduction	28
	6.2 Compilation of results and comparison with other sites	28
	6.3 Acidity and oxidation potential.....	29
	6.4 Salinity effects and major element hydrogeochemistry.....	30
	6.5 Minor element hydrogeochemistry.....	32
	6.6 Gold chemistry.....	33
	6.7 Mapping of the groundwater data	33

7	CONCLUSIONS	35
	7.1 Regolith and landform evolution.....	35
	7.2 Gold geochemistry.....	35
	7.3 Hydrogeochemistry	35
	7.4 Implications for exploration	36
	ACKNOWLEDGEMENTS	36
	REFERENCES	37
	APPENDICES.....	39

LIST OF FIGURES

Figure 1: Regional topography for the Federal area.....	2
Figure 2: Location of Federal Pit and other exploration areas at Woodcutters, with groundwater sample positions and the surface elevation also shown.....	2
Figure 3: Location and simplified geology of the Federal area (from Zhou and Phillips, 1998).....	3
Figure 4: Diagrammatic representation of method of calculating Au concentration from slices defined for the upper surface and for the unconformity.....	7
Figure 5: Calculated (A) regolith reliability, (B) unfiltered Au concentration and (C) filtered (> 60% reliability) Au concentration colour coded to reliability.....	8
Figure 6: Comparison of the regolith logging schemes for Federal.....	9
Figure 7: Weathering front (TOFR) elevation at Federal.....	9
Figure 8: BOCO elevation at Federal.....	10
Figure 9: Unconformity (BOA) elevation at Federal.....	11
Figure 10: Regolith stratigraphy, the SW wall of the Federal open pit.....	12
Figure 11: Regolith stratigraphy along a 1 km NW-SE traverse on the NE side of the Federal open pit.....	12
Figure 12: XRD patterns of untreated and glycerated saprolite sample.....	13
Figure 13: Transported overburden stratigraphy on the NNE wall of the Federal open pit.....	15
Figure 14: Three dimensional perspective views of the Au distribution, for different cut-off grades, Federal.....	17
Figure 15: Calculated Au grade for section across the orebody, Federal (40580N, looking NW).....	18
Figure 16: Calculated Au grade for section across the orebody, Federal (40480N, looking NW).....	18
Figure 17: Calculated Au grade for longitudinal section along the Federal orebody (looking SW).....	18
Figure 18: Calculated thickness of each regolith layer, Federal orebody.....	19
Figure 19: Mean Au concentration for each regolith layer, Federal orebody.....	19
Figure 20: Mean Au concentration vs. elevation, Federal orebody.....	20
Figure 21: Mean Au concentration vs. distance from the weathering front, Federal orebody.....	20
Figure 22: Mean Au concentration vs. distance from the transition/oxide zone boundary (BOCO) for the oxide and transition zones, Federal orebody.....	20
Figure 23: Associations of elements within the primary rock, Federal.....	21
Figure 24: Associations of elements within the saprock and saprolite, Federal.....	21
Figure 25: Associations of elements within the clay saprolite, Federal.....	22
Figure 26: Distribution of Au, Ca, Sr and Fe with depth through transported overburden, NE wall of the Federal pit.....	23
Figure 27: Mean Au concentration vs. distance from the unconformity for alluvium and oxide, Federal orebody.....	23
Figure 28: Mean Au concentration vs. distance from the surface for alluvium, Federal orebody.....	23
Figure 29: Eh vs. pH for groundwaters from Woodcutters and other sites.....	30
Figure 30: pH vs. TDS for groundwaters from Woodcutters and other sites.....	31
Figure 31: Potassium vs. TDS for groundwaters from Woodcutters and other sites.....	31
Figure 32: Dissolved Au concentration vs. Eh for Woodcutters and other Western Australian groundwaters.....	33
Figure 33: Dissolved Au distribution at Woodcutters, with the areas where average Au grades are greater than 50 ppb, the Federal Pit and the surface elevation also shown.....	34
Figure 34: Dissolved Mo distribution at Woodcutters, with the areas where average Au grades are greater than 50 ppb, the Federal Pit and the surface elevation also shown.....	34

1 INTRODUCTION

1.1 Location

The Federal deposit is located in the Woodcutters area, about 40 km NNW of Kalgoorlie (Figure 1) at 30°24' S and 121°24' E. Prospects within the tenement include (from SE to NW): Federal (now an open-cut mine), Grand, Exchange (combined with Grand in this report) and Criterion (Figure 2). Centaur Mining and Exploration Ltd wholly owns the Woodcutters tenement area, which has an identified resource (estimated as of 1997) of 5.37 Mt at 2.7 g/t Au.

No historic Au production is recorded on the tenement, but small workings occur at the Oriental mine area, approximately 2 km to the NW of the Federal deposit. In 1996, the first RAB program was undertaken at the Federal zone adjacent to a geochemical anomaly defined by the adjoining tenement holder. RAB drilling outlined a supergene anomaly that has led to the definition of the Federal zone by RC and DC drilling (Oxenburgh, 1997).

1.2 Geology and mineralization

The Federal deposit lies within the Norseman-Wiluna greenstone belt in the central part of the Eastern Goldfields Province of the Yilgarn Craton (Figure 3). Nearly 50% of the SW Eastern Goldfields Province is underlain by granite. Recent geological studies suggest there are two major events of granite magmatism, *i.e.* pre-regional folding (> 2.68 Ma) and post-regional folding (Witt and Davy, 1977). The younger granites normally form elongate domes in the cores of anticlines. Geochemical studies suggest that the parent melts of the granites were derived by hydrous melting of tonalite, granodiorite and monzogranite in a layered lower crust. The older granites occur as circular to ovoid shapes, with emplacement occurring 2.665-2.660 Ma. It is believed that they were emplaced during and immediately after a major tectonic event that included a regional compression (Witt and Davy, 1977).

The deposit occurs in the SW part of the Scotia granite pluton, which is one of the older granite group. It is located about 6 km from the greenstone contact (Figure 3). The broad mineralized zone strikes NW and dips 50-60° to the NE (Zhou and Phillips, 1998). Mineralization is hosted by two granitoid types, *namely* the slightly more mafic major phase of medium-grained granodiorite and a fine-grained monzogranite with less quartz. Hydrothermal alteration is extensively developed at the Federal deposit, with an epidote-muscovite distal alteration zone grading to epidote-muscovite-carbonate±biotite alteration to proximal muscovite-biotite-sulphide alteration. Sulphides commonly replace mafic minerals, *such as* hornblende and biotite. At the Federal deposit, Au is always associated with pyrite and occurs with quartz-pyrite veins, or as minor Au and sulphide veinlets along a fracture system.

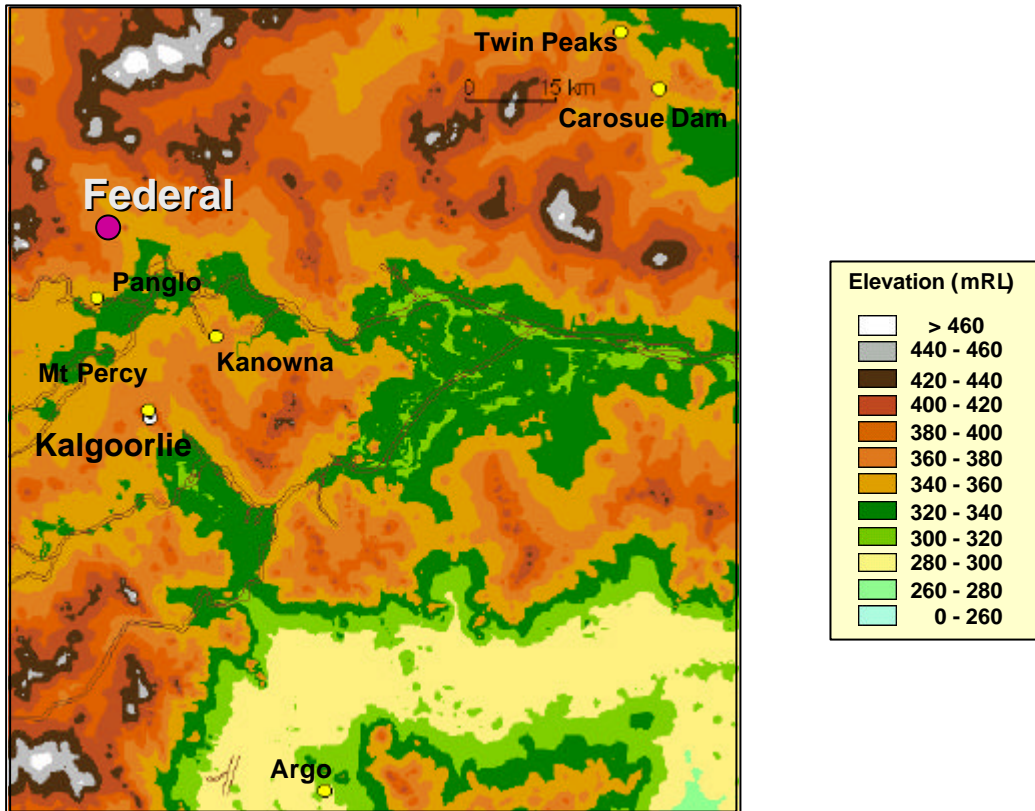


Figure 1: Regional topography for the Federal area.

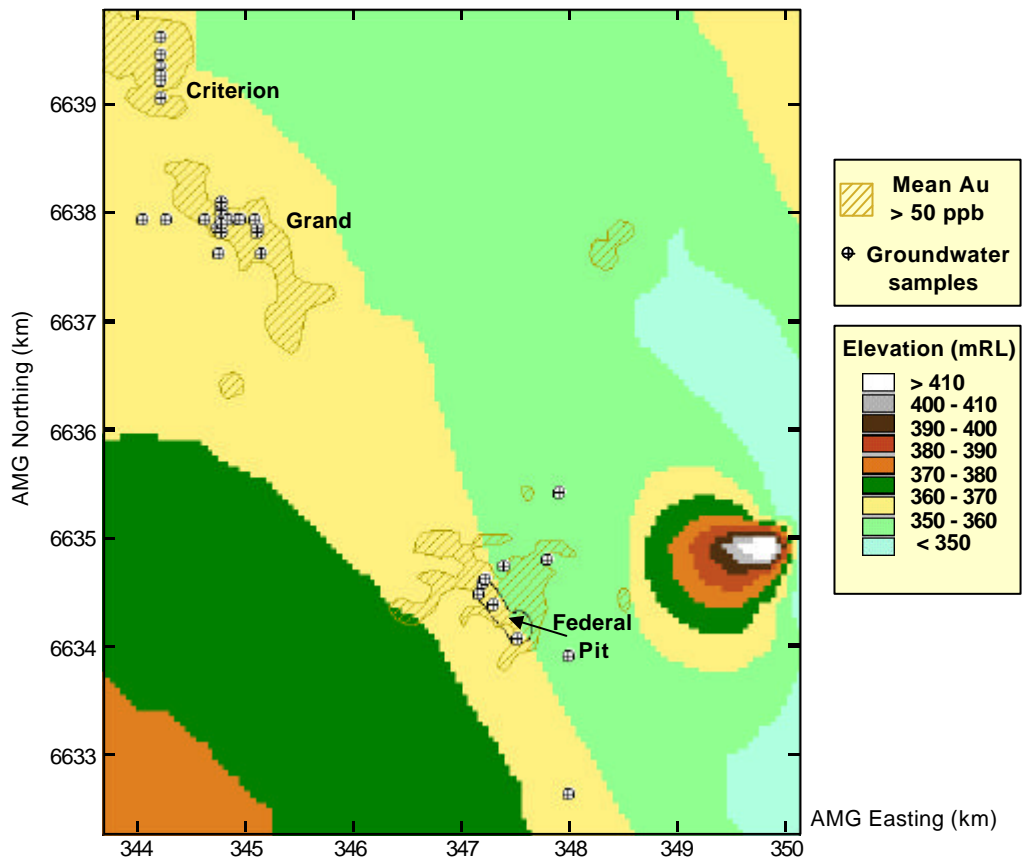


Figure 2: Location of Federal Pit and other exploration areas at Woodcutters, with groundwater sample positions (Section 2.1.5) and the surface elevation also shown.

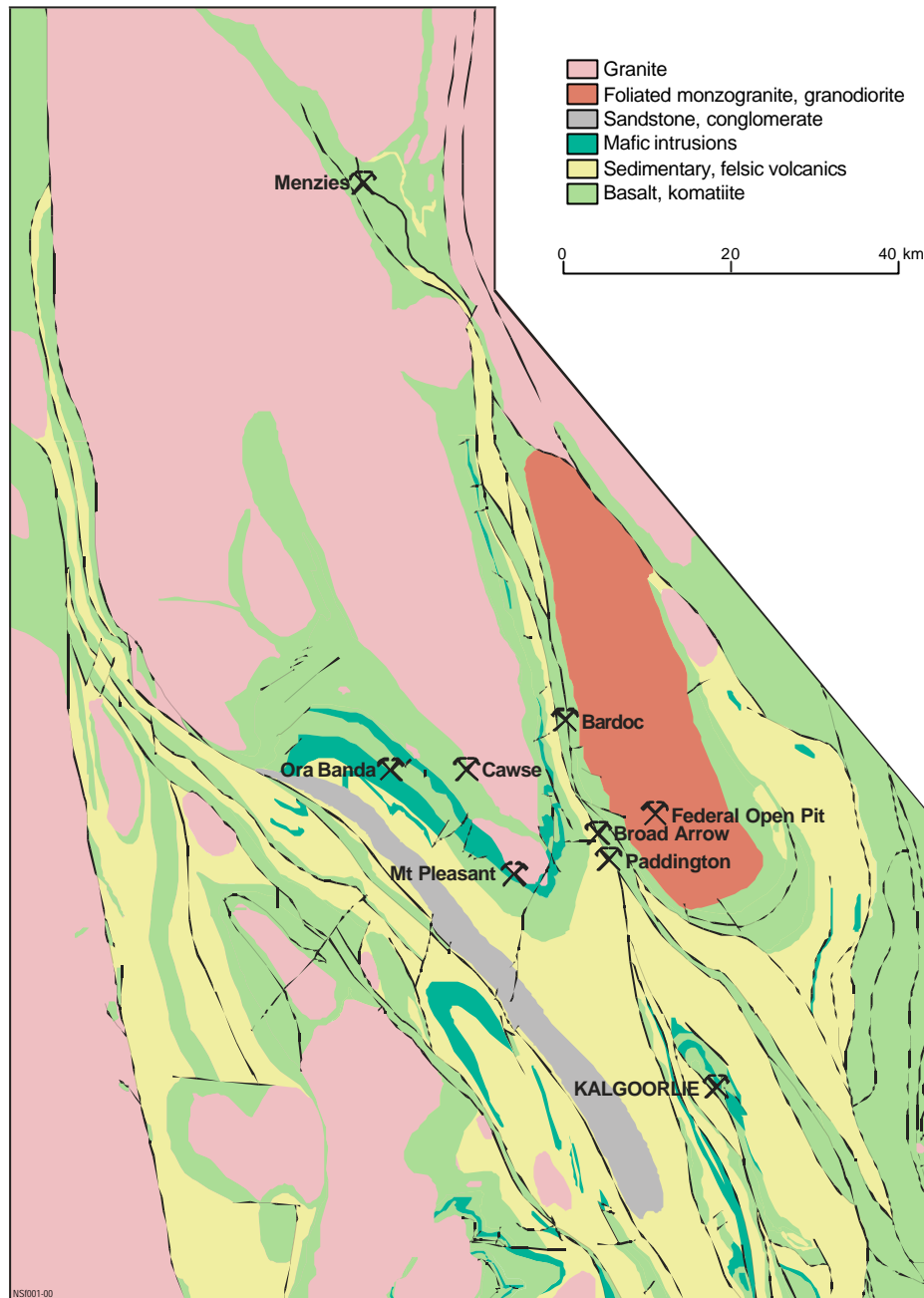


Figure 3: Location and simplified geology of the Federal area (from Zhou and Phillips, 1998).

1.3 Geomorphology, climate and vegetation

On a regional scale, the Federal deposit is situated within a SE sloping valley (Figure 1). Locally, it is located on a plain that gently slopes to the east (RL 366 - 353 m) (Figure 2).

The climate is semi-arid, with hot summers and cool to mild winters. Annual rainfall is 220-240 mm, with maximum rainfall during the winter period. However, there is a significant component of summer rainfall from occasional thunderstorms. The vegetation is a mixture of eucalypt and acacia woodlands, localised spinifex, saltbush and bluebush. Eucalypts dominate on calcareous soils and mulga (*Acacia aneura*) on acid red sandy clay soils.

2 STUDY METHODS

2.1 Sampling and analysis

2.1.1 Drill hole and open pit sampling

Three selected drill holes, WCUCD 411, WCUCD 431 and WCUCD 436 were sampled to a depth of 130 m for detailed regolith stratigraphy and geochemistry. Approximately 1-2 kg samples were taken from drill spoil for each metre and composited according to geology, weathering features and Au grades. In the Federal pit, bulk and trench samples were collected from the main residual regolith horizons and transported overburden. Large bulk samples (5-10 kg) were collected for Au grain studies from drill spoil and open pit.

2.1.2 Chemical analysis

All regolith and rock samples were dried at $< 40^{\circ}\text{C}$, jaw crushed, and a subsample taken for reference. The 200 g split samples were pulverized to $< 75\ \mu\text{m}$ in a hard carbon steel ring mill (Robertson *et al.*, 1996). A 10 g aliquot of each pulverized sample was analyzed by instrumental neutron activation analysis (INAA). Detection limits are as follows (ppm): Ca (10000); K (2000); Fe, Zr (500); Na, Ba, Zn (100); Rb (20); Ag, Se, Te, Cr, Mo (5); Br, Ce, U, W (2); As, Co, Cs, Ta (1); La, Eu, Yb, Hf, Th (0.5); Sb, Sm, Lu (0.2); Sc (0.1); Ir (0.02); Au (0.005) (Becquerel Laboratories Pty. Ltd.). X-Ray fluorescence spectroscopy (XRF) was conducted at CSIRO on fused discs (1.6 g sample and 6.4 g lithium borate flux) using a Philips PW1480 instrument. Detection limits were as follows (ppm): Na, Mg, Al, Si (100); Fe (50); Ti, Mn (30); P, Cl, Ba (20); Ce (15); S, K, Ca, Cr, Co, Cu, La, Ni (10); Pb, Rb, Sr, V, Y, Zn, Zr (5); Nb (4); Ga (3).

2.1.3 Mineralogical analysis

Selected pulverized samples were examined by X-ray diffraction at CSIRO using a Philips PW1050 diffractometer, fitted with a graphite crystal diffracted beam monochromator using $\text{CuK}\alpha$ radiation. Oriented clay aggregates were prepared using porous ceramic plates and treated with 2M MgCl_2 to saturate ion-exchange positions in smectites (Moore and Reynolds, 1997). Each sample was scanned over the range $2-65^{\circ} 2\theta$ at a speed of $2^{\circ} 2\theta/\text{min}$. Mineral identification was determined using software package Xplot for Windows, version 1.34. The smectite identification was verified by XRD analysis of the glycerol-solvated samples. XRD of formamide-treated samples was used to distinguish between kaolinite and halloysite (Churchman *et al.*, 1984).

2.1.4 Gold grain separation and analysis

Seven bulk samples with from saprolite, saprock and the primary mineralization were collected for separation of Au particles. Samples were dried and split, and subsamples washed with a non-ionic surfactant (0.01% Triton X-100). Gravity separation was performed on a Haultain Superpanner, a mechanized version of the prospector's pan. The panner consists of a 72 cm long, shallow, v-shaped trough, mounted on a 3 point suspension. The trough slope is variable. The trough is shaken by a cam that agitates the trough on each rotation. In addition, a variable frequency side shake with independently variable amplitude at each end can be applied. The Superpanner was set to a cam speed of 284 rpm and 7 mm axial vibration amplitude. A 10 mm side shake amplitude was applied at each end in opposing sense, to cause a rotational oscillation around vertical axis. The trough angle was varied during the treatment. After the dispersion was complete, the pulp was slowly introduced at the middle part of the trough during agitation. With increasing slope of the trough, a thin tail of heavy minerals was obtained in the top quarter of the trough. As fractionation progressed, the light mineral fraction was removed by suction into the collector and a new portion of the pulp was added. This cycle was repeated and the final tail of heavy minerals was collected into a small suction flask by vacuum. The trough was then thoroughly washed and wiped clean with damp tissue, until there was no discolouration, before the next sample was introduced.

The small, gram-size concentrate was transferred into the trough of a micropanner. This trough is 10 cm wide and 25 cm long and is provided with a changeable slope, cross-wise rocking and trough length direction vibration. A combination of varying slope angle and wash rate was used to separate Au from the other minerals. Gold particles >5 µm in diameter were recovered under a binocular microscope by a sticky needle and deposited on the slide on two-sided adhesive tape.

The morphology of Au grains and their size distribution were examined and measured using an optical microscope. The morphologies of selected particles were then examined by scanning electron microscopy (SEM). Their Ag content and the composition of neighbouring minerals were determined semi-quantitatively (limited by surface effects of the unpolished grains) using an energy dispersive detector. The SEM study was done in backscattered electron mode, using Philips XL40 instrument fitted with an environmental sample chamber (CSIRO laboratory). This permitted examination of samples without a conductive coating.

2.1.5 Groundwater sampling and analysis

Thirty six groundwater samples were collected on site from drill holes by pump sampler or as pit flows for five samples from the Federal pit in November 1998 and May 1999 (Figure 2). Included in this Figure are the areas where average Au grades are greater than 50 ppb, the Federal Pit and the surface elevation.

All groundwater samples were analysed for pH, temperature, conductivity and oxidation potential (Eh) at the time of sampling. A 125 mL aliquot was collected in a polyethylene bottle (with overfilling to remove all air) for HCO₃⁻ analysis by alkalinity titration in the laboratory. About 1.5 L of water was filtered on site through a 0.2 µm membrane filter. About 100 mL of the filtered solution was acidified [0.1 mL 15 M nitric acid], and analysed for:

- (i) Al, B, Ba, Ca, Cu, Cr, Fe, K, Mg, Mn, Na, Ni, P/I (distinction between P and I is difficult due to spectral overlap), S, Sc, Si, Sr, V and Zn by ICP-AES;
- (ii) Ag, As, Bi, Cd, Ce, Co, Ga, La, Li, Mo, Sb, Ta, W and Y by ICP-MS;
- (iii) total phosphate by the molybdenum blue colorimetric method (Murphy and Riley, 1962).

About 50 mL of the filtered water was collected separately, without acidification, and analysed for Cl by the Technicon Industrial method (Zall *et al.*, 1956).

A one litre sub-sample of the filtered water was acidified with 1 mL 15 M HNO₃, and a one gram sachet of activated carbon added. The bottle was rolled for eight days in the laboratory and the water discarded. The carbon was then analysed for Au by INAA at Becquerel Laboratories, Lucas Heights. The method was tested by shaking Au standards of varying concentrations, and in varying salinities, with activated carbon (Gray, unpublished data).

The solution species and degrees of mineral saturation were computed from the solution compositions using the program PHREEQE (Parkhurst *et al.*, 1980; described in detail in Gray, 1990 and Gray, 1991). The program determines the chemical speciation of many of the major and trace elements. To obtain highly accurate speciation data on a limited suite of the major elements (Na, K, Mg, Ca, Cl, HCO₃, SO₄, Sr and Ba), the specific ion interaction model, using the Pitzer equations, was applied, using the program PHRQPITZ (Plummer and Parkhurst, 1990). These programs calculate the solubility indices (SI) for each water sample for various minerals. If the SI for a mineral equals zero (empirically from -0.2 to 0.2 for the major element minerals such as halite or gypsum, and -1 to 1 for the minor element minerals), the water is regarded as being in equilibrium with that mineral, under the conditions specified. If the SI is less than zero, the solution is under-saturated with respect to that mineral, so that, if present, the phase may dissolve. If the SI is greater than zero, the solution is over-saturated with respect to this mineral, which can potentially precipitate from solution. Note that this

analysis only specifies possible reactions, as kinetic constraints may rule out reactions that are thermodynamically allowed. Thus, for example, waters are commonly in equilibrium with calcite, but may become over-saturated with respect to dolomite, due to the slow rate of solution equilibration and precipitation of this mineral (Drever, 1982).

Calculations of the SI values are important in understanding solution processes. They have particular value in determining whether the spatial distribution of an element is correlated with lithology or mineralization, or whether it is related to weathering or environmental effects. Thus, if Ca distribution is controlled by equilibrium with gypsum in all samples, the spatial distribution of dissolved Ca will reflect the SO_4 concentration alone and will have no direct exploration significance.

2.2 3D gridding, visualization and Au concentration calculations

Centaur Mining and Exploration Ltd supplied logging and geochemical data for modelling using the Mining Visualization System (MVS; © C Tech Corporation). Based on the logging data, four zones were delineated:

- (i) transported overburden;
- (ii) oxide zone, which includes all *in situ* material down to the “base of complete oxidation” (BOCO; Section 3);
- (iii) transition zone, lying between the BOCO and the weathering front;
- (iv) fresh rock.

Regolith boundaries (surface, unconformity, BOCO and weathering front) were gridded, “point” anomalies removed from the input data, and the data re-gridded. Although this filtering has the potential to bias the data, it was considered necessary to give coherent weathering horizons. For pictorial presentations of Au distribution, the data were pre-processed by a logarithmic transform (to base 10) of Au concentrations before gridding. Although this can affect the gridded magnitude of the main mineralization pattern, it enhances the detail of the subtle variations in Au concentrations in the supergene zone. For Au concentration calculations, untransformed data were used.

Two different sized areas were used for gridding, the orebody and the whole Federal area.

Stratigraphy was gridded with the KRIG_3D_GEOLOGY module within MVS. The geochemical data were then kriged in relation to these surfaces, using the KRIG_3D module. The maximum number of data points (within the specified reach) considered for the parameter estimation at a model node were set to 120. The horizontal/vertical anisotropy was set at 2.5 (*e.g.*, data points in a horizontal direction away from a model node influence the kriged value at that node 2.5 times more than data points an equal distance away in a vertical direction) and post-processing maximum set to 50 ppm Au. The grid cell size used was X:Y:Z - 10 m:10 m:3 m.

Gold concentrations were calculated with untransformed data, using the VOLUME_AND_MASS module in MVS. No attempt was made to model different bulk densities for the different units. As the Au grade data are as mass/mass rather than mass/volume, uniform density has only a minor influence on most calculations. The calculated concentrations do not compensate for leaching of mobile constituents: if half of the minerals have dissolved and been leached then Au grade will double because of residual concentration.

In addition, Au concentrations were calculated for slices of 3 m vertical thickness defined either by elevation (*e.g.*, 390-393 m RL) or distance from a regolith boundary (*e.g.*, 3-6 m above the unconformity).. Figure 4 illustrates nominal 3 m slices taken downwards from the unconformity, which become truncated downwards at the weathering front, as the analysis is set up not to include the next regolith horizon. While this method may be arithmetically correct, it can lead to over- or under-

estimations of concentrations as the slices get further from the reference transition (in this case the unconformity). This is because, ultimately, the slice being analyzed is not complete, again illustrated in Figure 4 as the slices becoming more and more truncated by the weathering front. Note that this is not a problem in calculation accuracy, but in the actual geometry of the study area. This can be expressed as a reliability factor, which is the mass of the slice divided by the mass of an untruncated slice (Figure 4). A reliability index of 85% indicates that the slice is 15% truncated.

As the reliability index decreases, significant errors can occur. Figure 5 shows the results of Au concentration measurement for each slice from the unconformity. Though the deeper slices are truncated (Figure 5a), they can still contain mineralized material, as in this example (Figure 4). Thus, a similar mass of Au is being divided by smaller and smaller amounts of regolith, which leads to anomalous Au concentrations (Figure 5b). In this example, the results indicate that the deepest slice has up to 440 ppb Au even though the “real” Au content is invariant at 80 ppb, except for the leached zone at the top of the *in situ* regolith.

When all the slices with reliability indices less than 60% are removed, the remaining results can be coded for reliability (Figure 5c). A much clearer picture of the Au trends appears, illustrating the depletion at the unconformity. Note that this example is for the maximum possible overestimation of Au grade (the maximum overestimation = $100 \div \text{reliability}$: e.g., when reliability is 60%, maximum overestimation is 1.67; when reliability is 90%, maximum overestimation is 1.11). In other cases underestimation can occur for low reliability samples (due to truncated intersection with mineralization). In summary, those samples with reliabilities less than 80% are suspect (but can still be valuable if treated with caution), whereas those with reliability less than 60% should generally not be used.

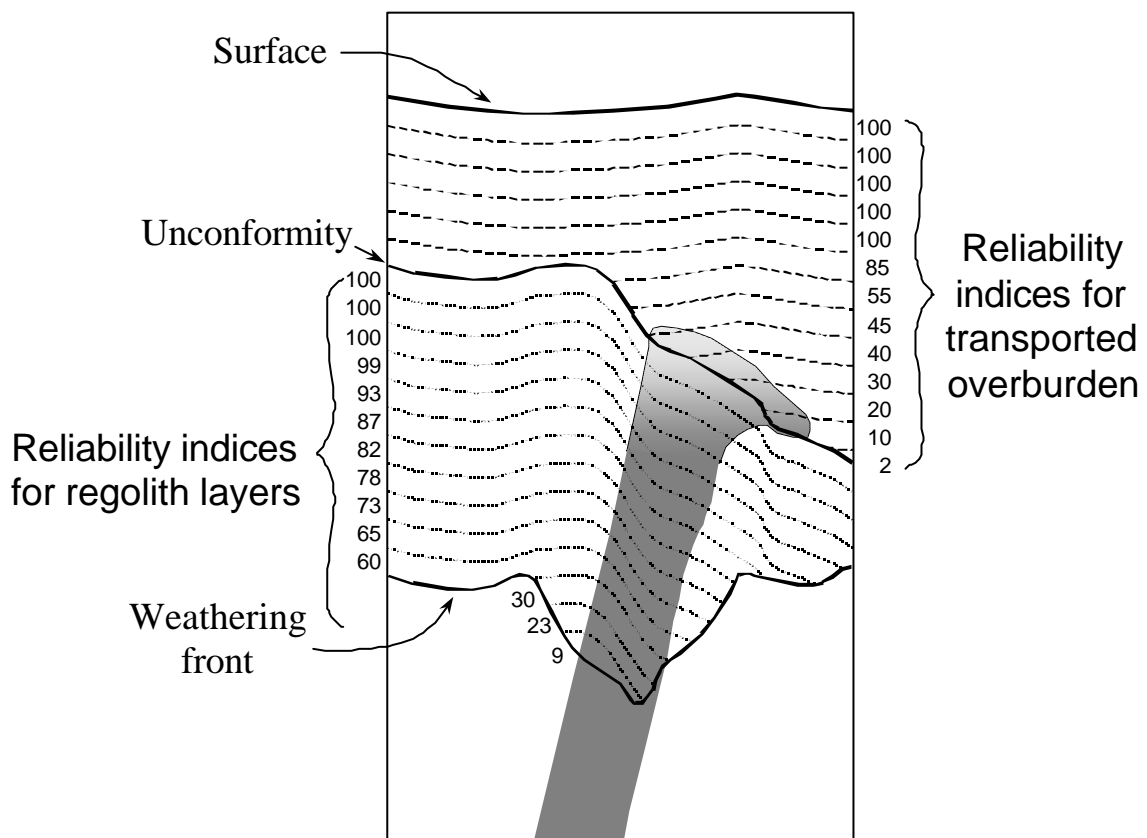


Figure 4: Diagrammatic representation of method of calculating Au concentration from slices defined for the upper surface and for the unconformity.

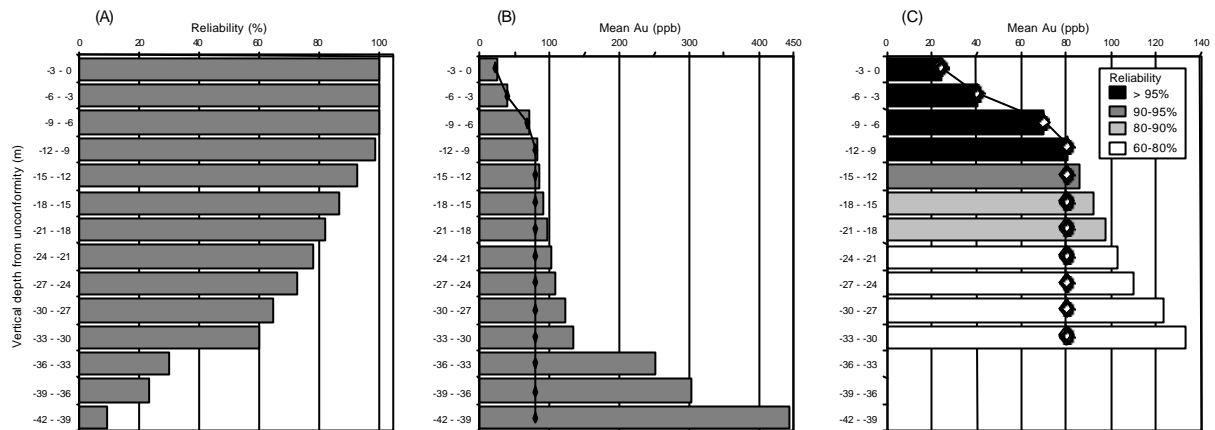


Figure 5: Calculated (A) regolith reliability, (B) unfiltered Au concentration and (C) filtered (> 60% reliability) Au concentration colour coded to reliability. Diamonds represent expected Au concentration. Data based on situation represented in Figure 4.

3 REGOLITH STRATIGRAPHY

3.1 Comparison between Centaur and CRCLEME logging

The regolith stratigraphy of the Woodcutters area was studied using computer 3D visualization of the exploration data and CRCLEME logging of the Federal open pit and of selected drill holes. In the Federal, Grand and Criterion prospects a total of 23, 15 and 8 drill holes, respectively, were logged in the field from RC and RAB drill cuttings. Regolith stratigraphy was studied in detail on 3 selected drill holes (WCUCD 411, WCUCD 431 and WCUCD 436) at Federal, using wet sieving, XRD and multi-element geochemistry. The stratigraphy of the residual profile and transported overburden were also studied in the Federal open pit.

The database on regolith logging for the Federal area (6633300 - 6635800 mN, 346400 - 348900 mE) containing the data on 4000 drill holes was analysed using MVS software package. Elevation maps of the major regolith transitions and maps of regolith unit thicknesses were generated and discussed below.

Three major regolith boundaries are defined by Centaur Mining and Exploration Ltd, as follows:

1. Base of alluvium (BOA) separating transported overburden and residual regolith;
2. Base of complete oxidation (BOCO) above which the regolith contains negligible unweathered rock fragments;
3. Weathering front (TOFR) separating regolith and fresh rocks.

Two major logging schemes with a combination of lithological and regolith codes were used by Centaur Mining and Exploration for regolith stratigraphy. To further understand the position and sense of major regolith boundaries, the CRCLEME and Centaur logging were compared, with correlation between regolith units shown in Figure 6. Comparisons show that the BOCO is mostly located at the transition from the clay saprolite to the saprolite, but does vary up and down in the profile. This variability makes comparison of Centaur and CRCLEME regolith data difficult. Therefore, the general terms for the regolith units as defined by Centaur Mining and Exploration Ltd, namely “oxide zone” (between BOA and BOCO) and “transition zone” (between BOCO and TOFR) were used to interpret the results of 3D modelling on regolith stratigraphy and Au geochemistry in this report.

Centaur Mining and Exploration				CRC LEME	
Previous Schemes		Current scheme			
1 st scheme	2nd scheme				
Alluvium	Alluvium	Alluvium	BOA	Transported overburden	
Clay saprolite	Saprolite	Oxide zone	BOCO	Mottled zone Clay saprolite	
Saprolite	Strongly, moderately and slightly weathered rock	Transition zone	TOFR	Saprolite	
Weathered rock				Saprock	
Fresh rock	Fresh rock	Fresh rock		Fresh rock	

Figure 6: Comparison of the regolith logging schemes for Federal.

3.2 Centaur regolith stratigraphy

In the Federal area, the regolith cover varies widely in thickness. The weathering front is deepest along the NW striking mineralized zone, reaching a depth of 70 - 75 m (285-290 mRL) with a mean depth of 60 m (Figure 7). Away from mineralization, the weathering front is commonly 45 to 50 m in depth, with rising to 25 m below the surface east and south of the mineralized area. This is possibly due to a lithological change from medium-grained granodiorite to a more resistant, fine-grained monzogranite.

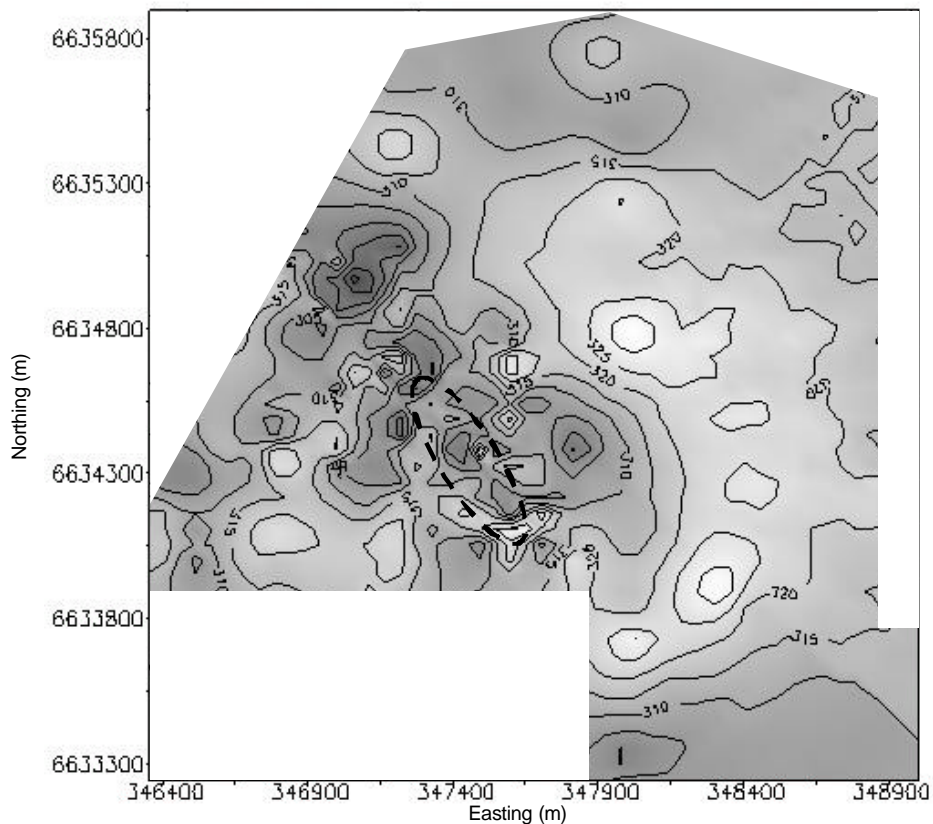


Figure 7: Weathering front (TOFR) elevation at Federal. The dashed line marks position of the open pit.

The major regolith boundaries identified are the weathering front (TOFR), transition/oxide zone boundary (BOCO) and the unconformity (BOA), with the four major units being fresh rock, transition zone, oxide zone and transported overburden (Figure 6).

The transition zone is 15-20 m thick in the unmineralized area, increasing to 40-45 m over the mineralization (thickness maps of the regolith zones are available with the accompanying CD). The BOCO elevation map shows a 10-15 m deep linear depression striking NE across the mineralized trend. Deepening of the BOCO down to 35 m occurs where the mineralized trend meets the NE trend (Figure 8).

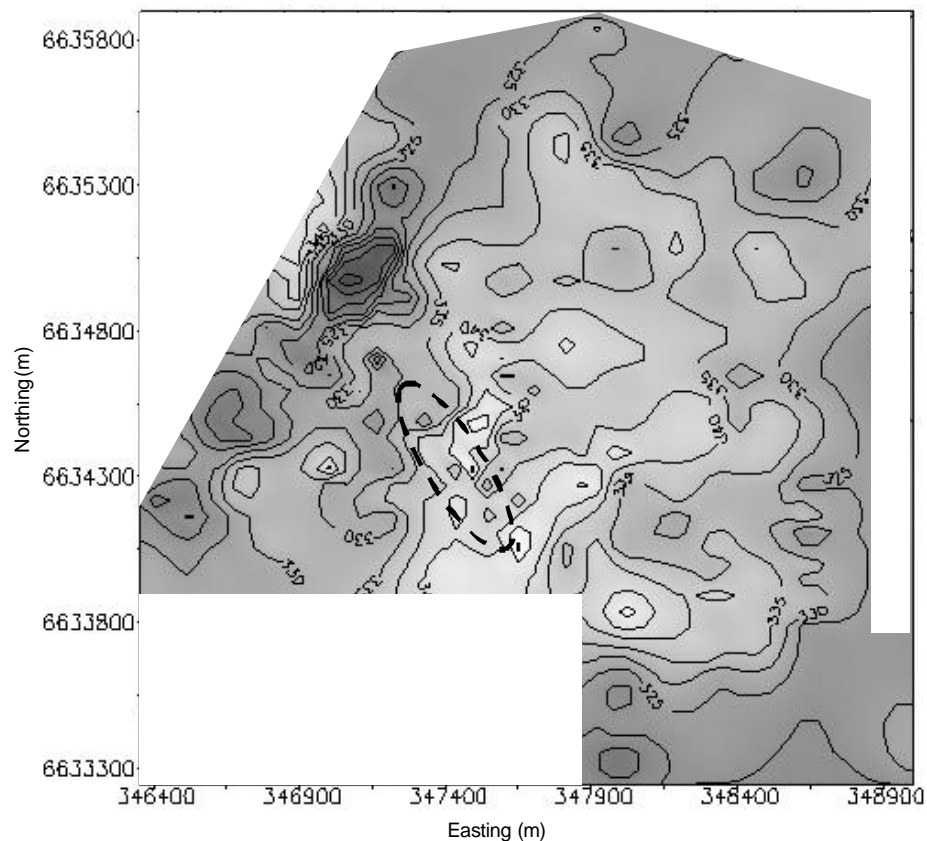


Figure 8: BOCO elevation at Federal. The dashed line marks position of the open pit.

The oxide zone is commonly 10-20 m in thick, increasing to 30 m along the mineralized trend. It reaches a maximum thickness of 40 m in the local area at 6635000 mN and 347050 mE.

Transported overburden is 2-10 m thick in the unmineralized area, increasing to 16 m over the NW part of the mineralized zone. Along the mineralized structure to the SE, the transported overburden decreases to 2 m in thickness. The unconformity generally follows to the surface, except for local deepening to 4 m along the mineralized structure (Figure 9). This depression is presumably due to contraction of the deeper weathered regolith over the mineralization.

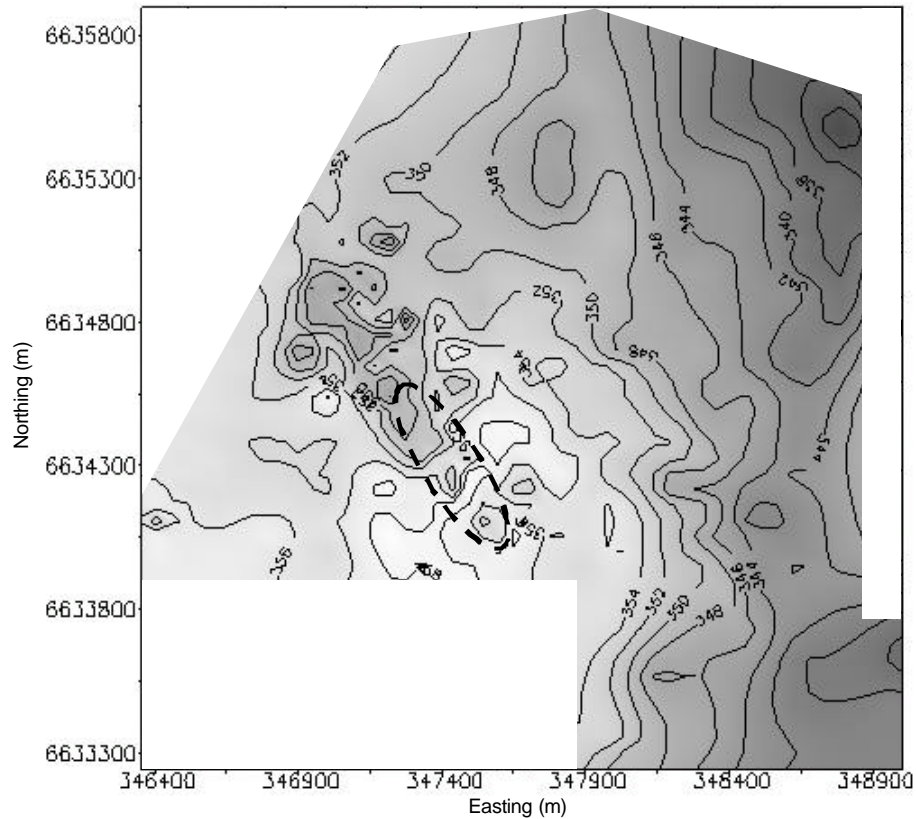


Figure 9: Unconformity (BOA) elevation at Federal. The dashed line marks position of the open pit.

3.3 CRCLEME regolith stratigraphy

CRCLEME's regolith logging was based on field logging and XRD analysis, with typical XRD patterns shown in Appendix 2, Figure A2.1. The complete residual profile over granitoids at Federal consists of saprock, saprolite, clay saprolite and mottled zone (Figure 10).

Logging of drill holes along a 1 km long NW traverse, 200-300 m NE of the Federal open pit, shows a decrease in the thickness of residual regolith and transported overburden to the SE (Figure 11). The residuum thickness and structure in the Grand exploration area, 3 km NW, are very similar to Federal, being 55-65 m thick, with saprock, saprolite, clay saprolite and mottled zone. At Criterion, 6 km NW of Federal, the regolith is slightly thinner (50 m), with similar regolith stratigraphy.

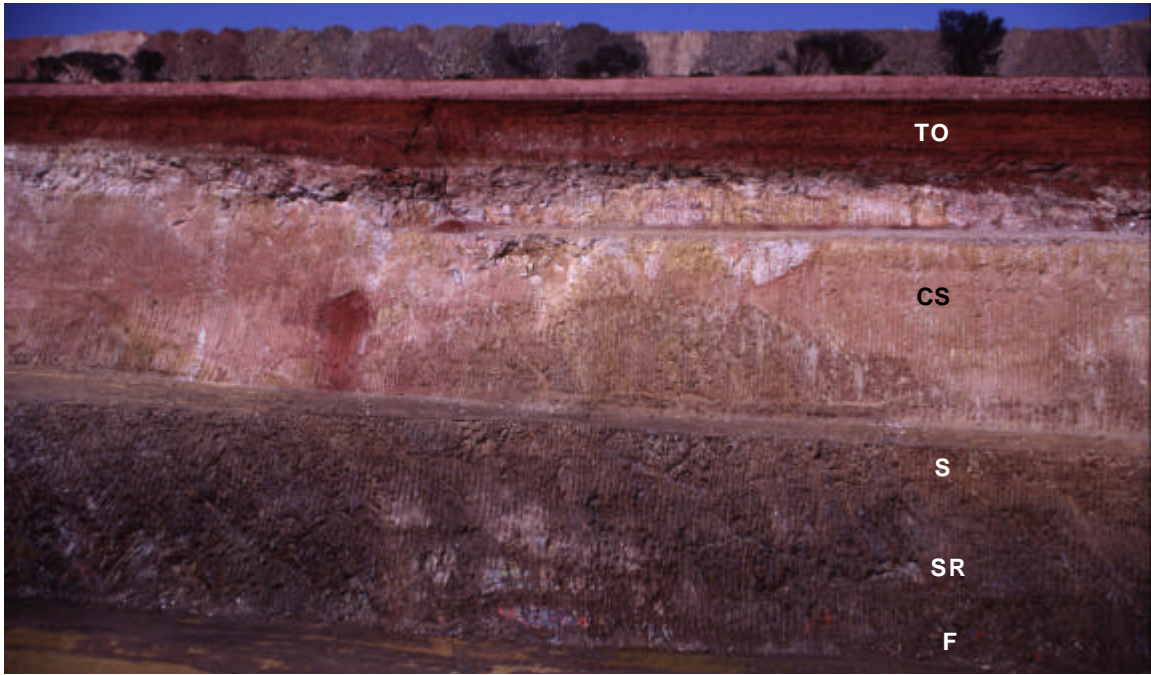


Figure 10: Regolith stratigraphy, the SW wall of the Federal open pit. Key: F – fresh rock, SR – saprock, S – saprolite, CS – clay saprolite, TO – transported overburden.

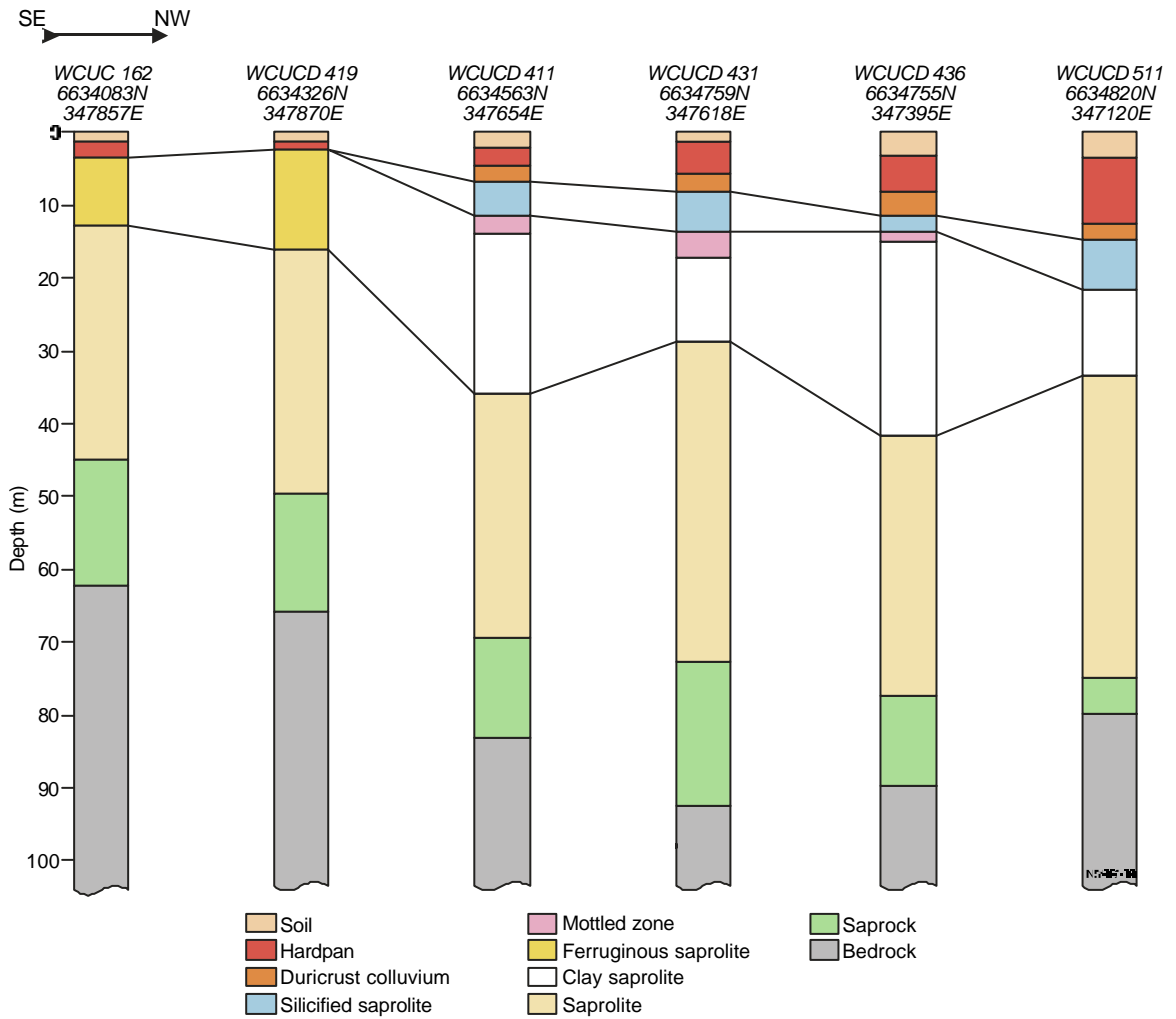


Figure 11: Regolith stratigraphy along a 1 km NW-SE traverse on the NE side of the Federal open pit.

Fresh rock

There are two major lithologies at Federal: granodiorite and monzogranite (Zhou and Phillips, 1998). The granodiorite is dark grey to grey, medium-grained (average 2-3 mm) felsic intrusive rock, with abundant biotite, hornblende, plagioclase, K-feldspar and quartz with minor titanite and tourmaline. Biotite is commonly replaced by muscovite and pyrite. Plagioclase and feldspar are largely replaced by epidote and muscovite. The monzogranite is pinkish-to-grey, fine- to medium-grained (average 0.5-1.5 mm) rock, consisting of K-feldspar, plagioclase, quartz and biotite, with minor hornblende, titanite and tourmaline. It has been substantially altered with biotite replaced by chlorite and plagioclase and feldspar replaced by muscovite. Epidote alteration is relatively weak compared to that in the granodiorite.

Saprock

Saprock is grey to grey-creamy solid unit, 5-20 m thick, with weak ferruginization along fractures. It contains minor smectite, identified by XRD analyses of glycerol-solvated, oriented samples (Figure 12).

Saprolite

The transition from saprock to saprolite is gradual. The main features of saprolite are grey-creamy and greenish-creamy colour and increased clay content. Smectite becomes more abundant (Figure 12) due to weathering of hornblende and feldspar. In the upper part of the unit, kaolinite appears as a minor mineral. The saprolite is 34-45 m thick.

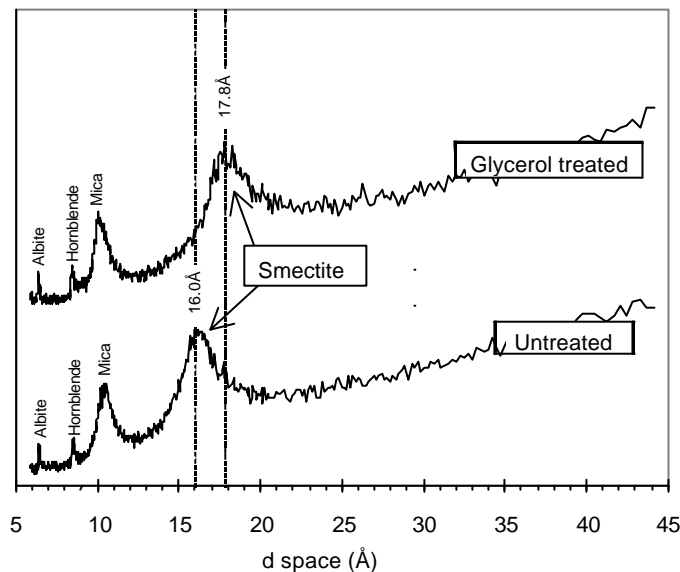


Figure 12: XRD patterns of untreated and glycerated saprolite sample (WCUCD 431, 40-41m depth).

Clay saprolite

This zone comprises clay-rich material with rock fabric retained and formally represents the upper part of the saprolite. The transitional zone from saprolite to clay saprolite takes place over 1-2 m. Above the transition, the regolith is clay-rich and coarse solid fragments diminish, with a change in colour from creamy to pale-greyish and white. Occasionally, ferruginous clay saprolite occurs instead of pale clay. Kaolinite becomes an abundant mineral, with minor smectite and Fe oxides. Concentrations of K, Na, Zn, Co and REE are sharply reduced in the clay saprolite with supergene accumulation of all REE and Sc at the base of the zone. These depletion/enrichments are presumably due to decomposition of K- and Na-feldspars, which are the principal hosts for these elements, with some concentration of REE and Sc at the regolith boundary. The clay saprolite is generally 12-27 m thick.

Mottled zone

This occurs as local lenses above the clay saprolite. It comprises purple, red and white clays, composed mainly of kaolinite, hematite and goethite, with coarse quartz and muscovite retained in this zone. The mottled zone is up to 10 m thick. The top few metres of the residual profile below an unconformity are silicified and retain the original rock fabric.

3.4 Transported overburden

3.4.1 Transported overburden stratigraphy

Transported overburden covers all the Woodcutters area and ranges from 2 to 10 m in thickness. The stratigraphy of the overburden is similar for the whole area, with some variations in thickness. The overburden consists of (from bottom to top): duricrust colluvium, silicified colluvium, hardpanized colluvium and soil.

The unconformity appears to occur at the contact between duricrust colluvium and the underlying silicified clay saprolite. Observations that support this hypothesis include:

1. The contact of silicified clay saprolite and duricrust colluvium is sharp without any gradual transition.
2. The fabric changes sharply at the contact, from relic granitic fabric in the silicified clay saprolite to unclear, subhorizontal bedding in duricrust colluvium.
3. A discontinuous stone line composed of silicified saprolite fragments occurs above the residual silicified saprolite.
4. Quartz rounded pebbles are observed in the duricrust colluvium.
5. Discriminant analysis of geochemical data suggests that the duricrust colluvium is part of the transported overburden (Section 3.4.2).

Duricrust colluvium

This is consolidated light-brown to creamy-brown porous rock, composed mostly of ferruginous nodules and pisoliths in a sandy matrix, cemented by silica, kaolinite and dolomite, with minor Fe oxides, calcite and smectite (Appendix 2, Figure A2.2). Pisoliths (1-2 cm in diameter) are commonly composed of quartz-hematite fragments with a thin yellow to yellow-greenish goethite cutan. The duricrust colluvium unit ranges 1.0 - 2.5 m in thickness.

Silicified colluvium

It is indurated, light to reddish brown rock composed of sand, sandy loam and gravel, cemented mostly by silica and minor clay. The colluvium is 2 - 6 m thick.

Hardpanized colluvium

This is indurated red to brown, porous laminated rock with a sandy to sandy loam texture and platy structure. The material progressively decreases in hardness upwards. The hardpanized colluvium is composed mainly of sand grains cemented by silica, aluminosilicates and Fe oxides. Some subhorizontal hardpan layers are rich in magnetic, black Fe oxide nodules. Manganese oxides are common as coatings along fractures. The upper layers of the hardpan are calcareous (up to 25% CaO) to a depth of 6 m, with fine-grained calcite and dolomite dispersed in the matrix and also occurring as calcrite nodules up to 2 cm in diameter, commonly at 1 - 3 m depth. The hardpan is 2 - 5 m thick.

Soil

This is sandy to sandy clay loam, weak to moderately calcareous with some coarse fragments of slightly weathered granites. Quartz, kaolinite and calcite are the principal minerals, with minor muscovite, Fe oxides and albite. The soil is up to 2 m thick.

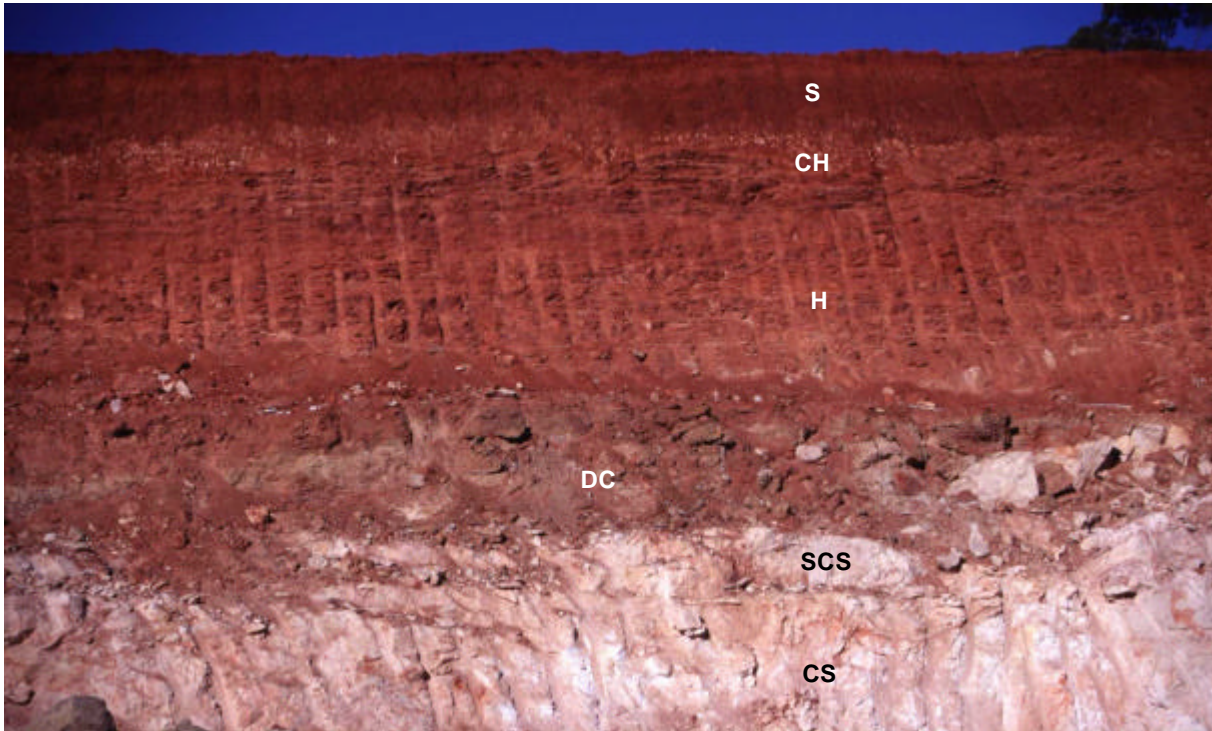


Figure 13: Transported overburden stratigraphy on the NNE wall of the Federal open pit. Key: CS – clay saprolite, SCS – silicified clay saprolite, DC – duricrust colluvium, H – hardpanized colluvium, CH – calcareous hardpan, S – soil.

3.4.2 Discriminant analysis and geochemical characterization of transported overburden units

Discriminant analysis was used to support logging of the unconformity and main sediment units. Geochemical characterization of the transported overburden units was performed using multi-element data on the Federal deposit for 64 samples, obtained from CRC LEME PhD student Annamalai Mahizhnan (Mahizhnan, 2000), combined with small data set for 9 samples on drill hole WCUCD 431 (Appendix 4, Table A4.1). Statistical treatment of the geochemical data was performed using the STATISTICA software package, version 5.0. For discriminant analysis raw data were normalised where required (Au, Cl and Br) using a log transformation. Discriminant analysis was performed in the forward stepwise mode, with significant canonical variates plotted as 2D graphs (Appendix 4, Figures A4.4-A4.5)

Soil

Soil is slightly enriched in Ca, Mg, K, Cu and Zn, compared to the other transported materials and saprolite. Calcium and Mg occur as carbonates, mainly calcite. High K concentrations correspond to the presence of muscovite and albite. Zinc correlates positively with K (Appendix 4, Figure A4.2) and appears to occur in aluminosilicate structures.

Hardpanized colluvium

It is slightly enriched in Zn, Co and Cr compared to the other sediments. The mean Fe concentration (8.8% Fe₂O₃) is slightly higher than that in cemented colluvium (6.4%); the Al values are similar.

Silicified colluvium.

The mean Si concentration is high (65.3% SiO₂) in this unit, but is only 4% less than that in the silicified saprolite (69.4% SiO₂). This is due mainly to the presence of quartz sand in the colluvium. Iron, Mn, Ca, Zn, Zr and Hf abundances are generally low.

Duricrust colluvium

This is the most ferruginous unit (15.2% Fe₂O₃). Thorium, V, As and, to a lesser extent, Sc and Pb concentrations are higher in this unit relative to the other units because of their association with Fe oxides.

Clay saprolite and silicified clay saprolite

These units have high Al and low Fe, Ca, Mg, Cu, Ni, Cr, Sc and As concentrations compared to the transported materials. In these two units, Si and Ba abundances are higher in the silicified clay saprolite, with higher Na and Cl concentrations in the saprolite. The latter elements presumably occur as halite. Higher Ti, Zr and Hf concentrations in the silicified clay saprolite are due to one outlier.

Zn-Sc and Fe₂O₃-Ni plots distinguish between residual materials (*i.e.*, silicified clay saprolite and clay saprolite) and major units of the transported overburden (*i.e.*, soil, hardpanized and silicified colluvium, and duricrust colluvium) at the Federal deposit (Appendix 4, Figures A4.2-A4.3). The Zn-Sc plot discriminates (with some overlap) between soil, duricrust colluvium, residual materials and hardpanized plus silicified colluvium groups.

Discriminant analysis was used to optimise the separation of the residuum and sediments at the Federal deposit. Canonical analysis gave a good separation, especially between residual regolith materials and transported overburden (Appendix 4, Figures A4.4-A4.5). There is good discrimination within the transported overburden, although overlaps between hardpan and colluvium in the CV1-CV2 plot, and between duricrust colluvium and soil in the CV1-CV3 plot occur. The most useful elements appear to be Al, Zn, Sc, Th and Zr.

Good discrimination between *a priori* defined regolith and sediment units at Federal confirms correct logging and geochemical difference between the transported overburden units. Raw and summary geochemical statistics for major transported materials and residual saprolite are tabulated in Appendix 4, Tables A4.1-A4.6 and are shown as Box and Whisker plots in Appendix 4, Figure A4.1.

4 GOLD GEOCHEMISTRY

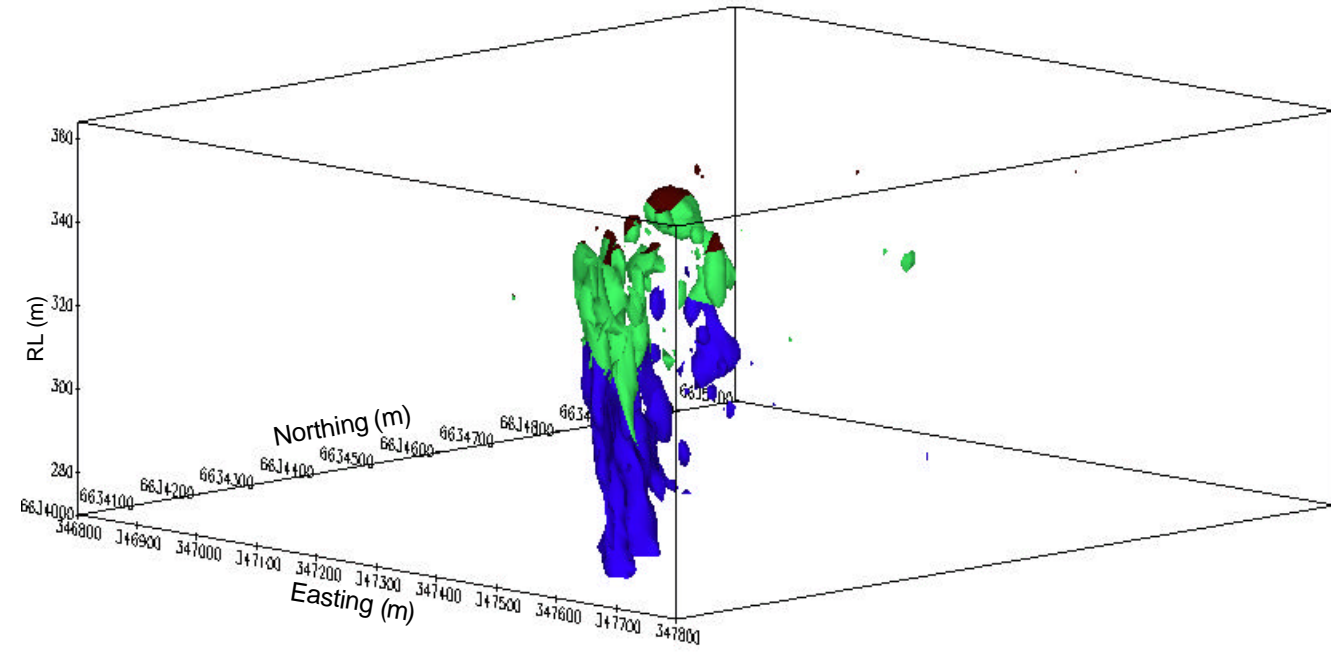
4.1 Gold in residuum

4.1.1 Patterns of gold distribution

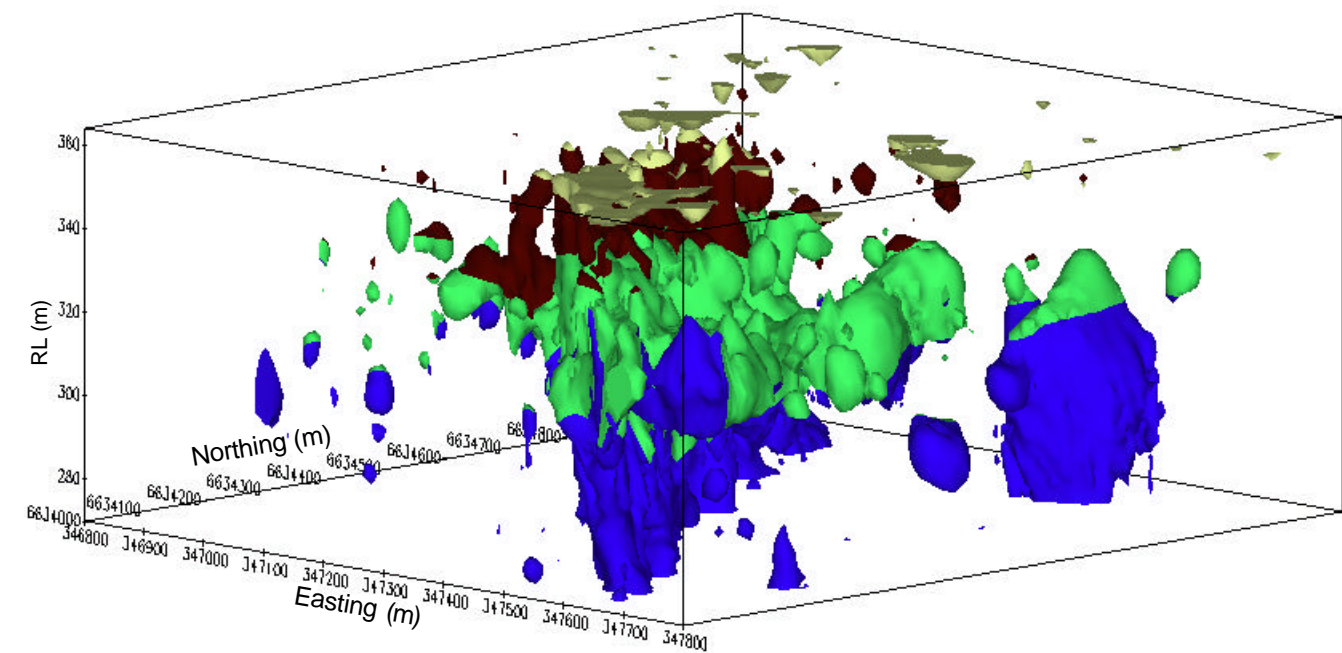
The Au distribution at Federal was studied using 3D cut-off diagrams and geochemistry slice diagrams (Section 2.2). The trend of primary mineralization in regolith and bedrock is seen clearly using a 500 ppb cut-off (Figure 14A). The sheet-like ore zone strikes NW and dips 50 - 60° to NE. The oxide zone and transported overburden have lower (up to 200 ppb Au) concentrations over the mineralized structure. In the regolith around the mineralized zone, Au concentrations are generally less than 60 ppb. Subhorizontal Au-rich (up to 100-150 ppb) patches occur at two levels: at the top of the oxide zone and near the weathering front. At the weathering front, the dispersion halo extends as a patchy cover up to approximately 400 m to the east, at a 60 ppb cut-off (Figure 15 and Figure 16). However, much of this halo is located above the slightly (up to 30 ppb) mineralized primary rocks (Figure 14D), suggesting that this enrichment is due to a combination of residual and absolute Au accumulations, with transport of Au possibly following fault structures.

The upper enrichment is several metres below the transition/oxide zone boundary (BOCO). Longitudinal sections through the mineralized zone show enrichment within the orebody at the BOCO. They form a chain of local Au-rich (up to 1 ppm) spots, and a pronounced decrease in Au abundance above the boundary, due to depletion (Figure 17).

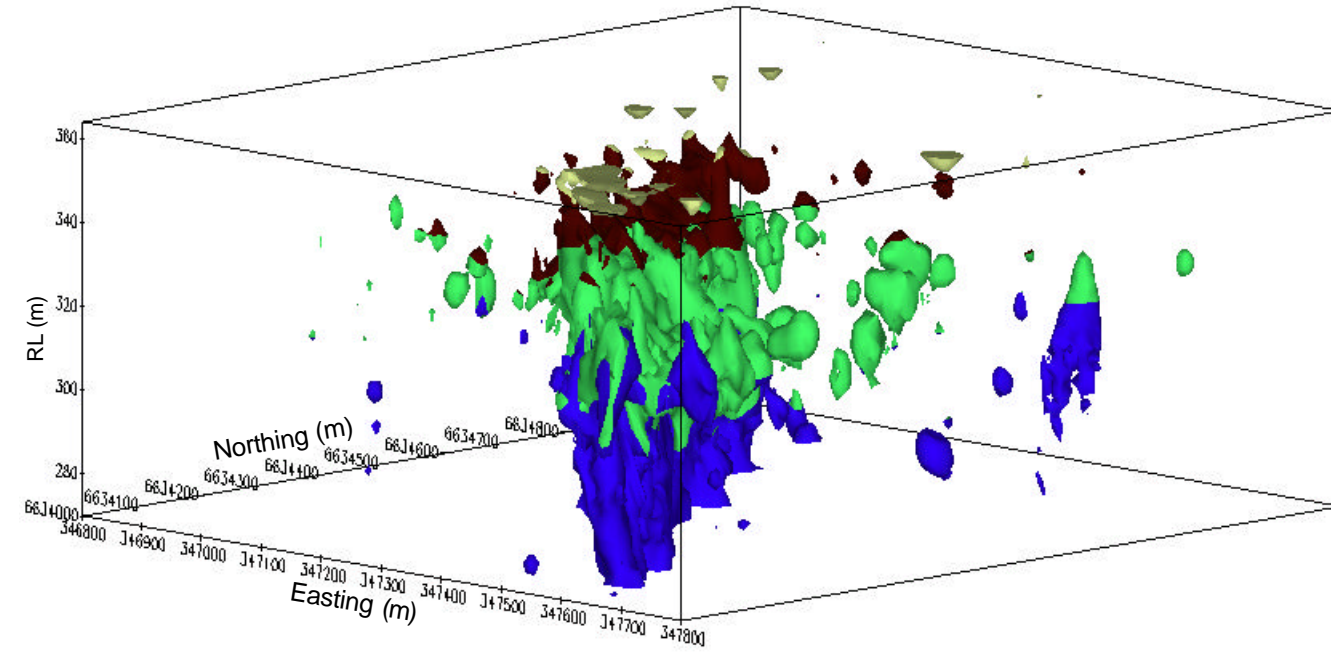
(A) 500 ppb Au cut-off



(C) 60 ppb Au cut-off



(B) 90 ppb Au cut-off



(D) 30 ppb Au cut-off

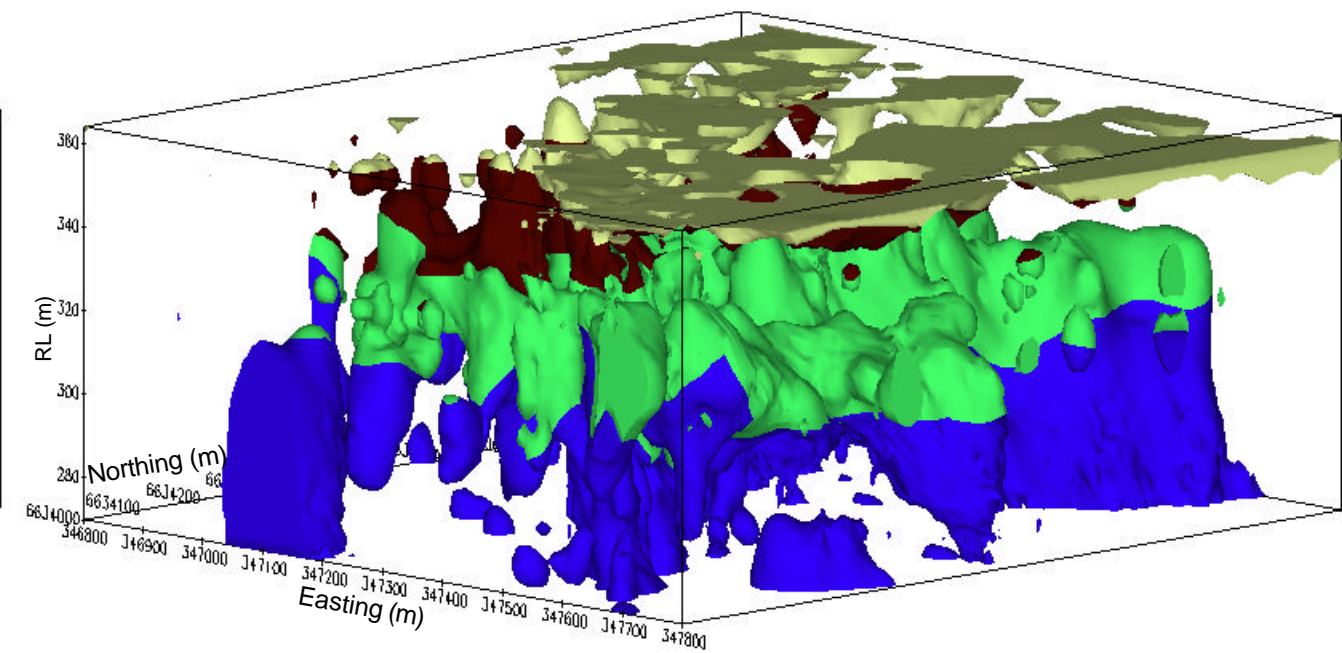


Figure 14: Three dimensional perspective views of the Au distribution, for different cut-off grades, Federal. Key: blue – fresh rock, green – the transition zone, brown – the oxide zone, yellow-green – transported overburden.

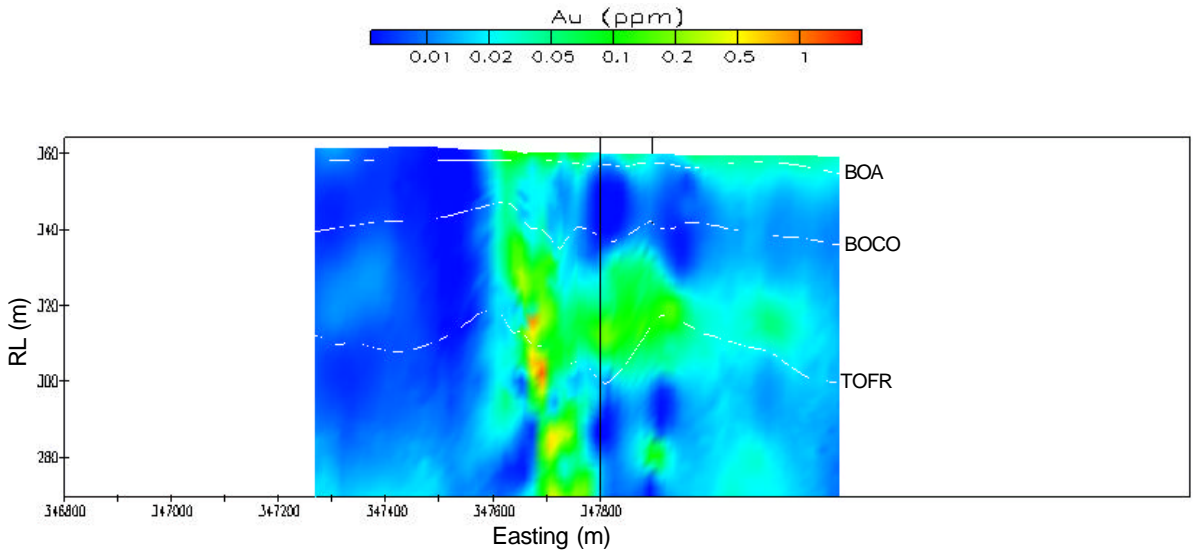


Figure 15: Calculated Au grade for section across the orebody, Federal (40580N, looking NW).

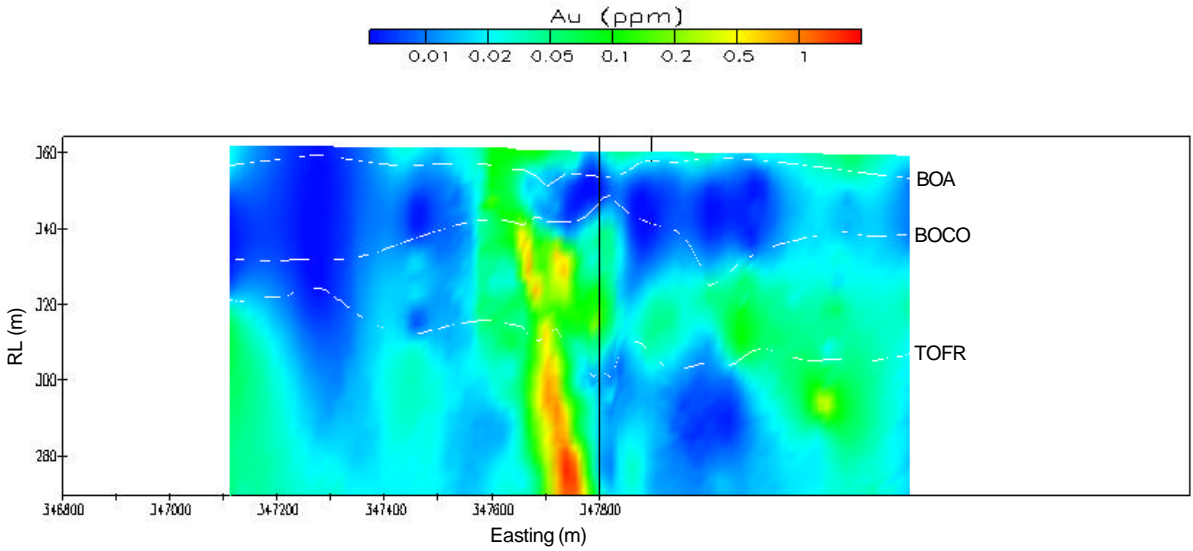


Figure 16: Calculated Au grade for section across the orebody, Federal (40480N, looking NW).

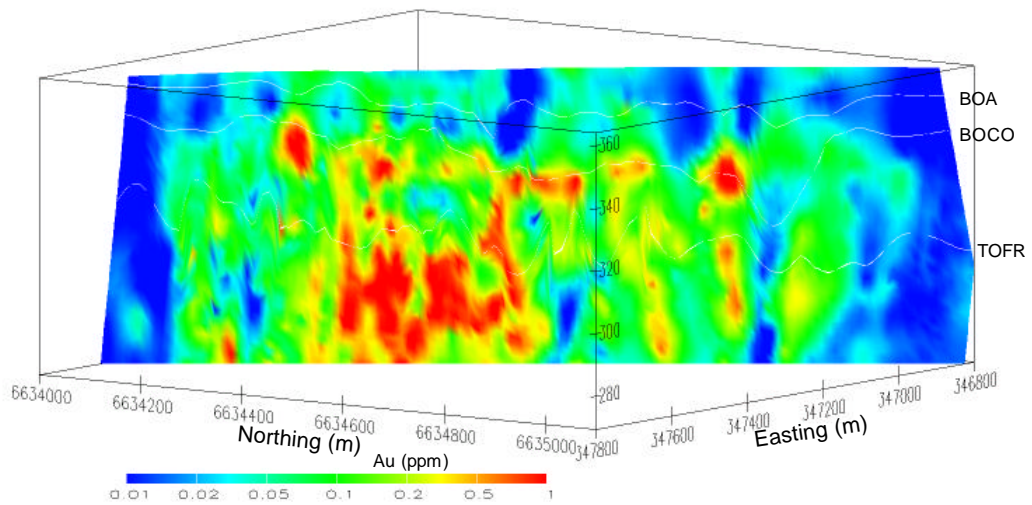


Figure 17: Calculated Au grade for longitudinal section along the Federal orebody (looking SW).

4.1.2 Gold concentration calculations

Gold concentrations for individual slices were calculated for the orebody itself and the entire Federal area (6633300 - 6635800 mN, 346400 - 348900 mE). Calculations show similar results for both data sets. The data for the whole area have lower calculated Au concentrations and only results for the orebody are discussed below.

Over half the regolith is logged as the transition zone (Figure 18), consistent with this unit representing the entire saprolith (Figure 6). Calculations of the mean Au concentrations in the major regolith units (Figure 19) show an apparent enrichment in the transition zone (514 ppb) compared to primary rock (281 ppb). The oxide zone has a much lower mean Au concentration (139 ppb) compared to primary rock indicating Au depletion. The transported overburden is low in Au (45 ppb) compared to the residuum and the bedrock.

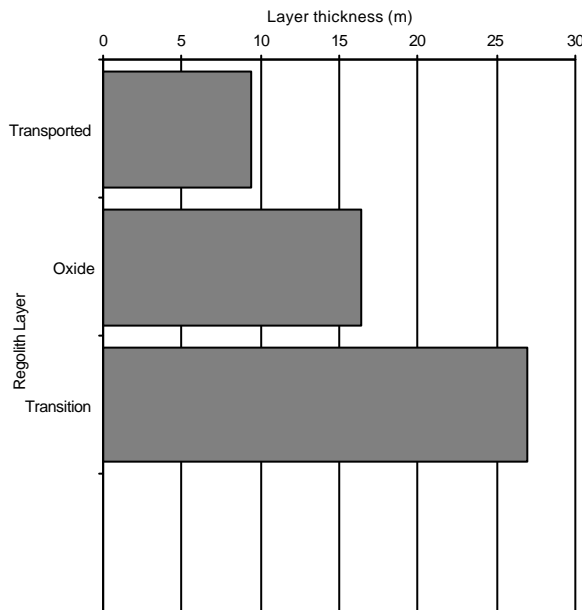


Figure 18: Calculated thickness of each regolith layer, Federal orebody.

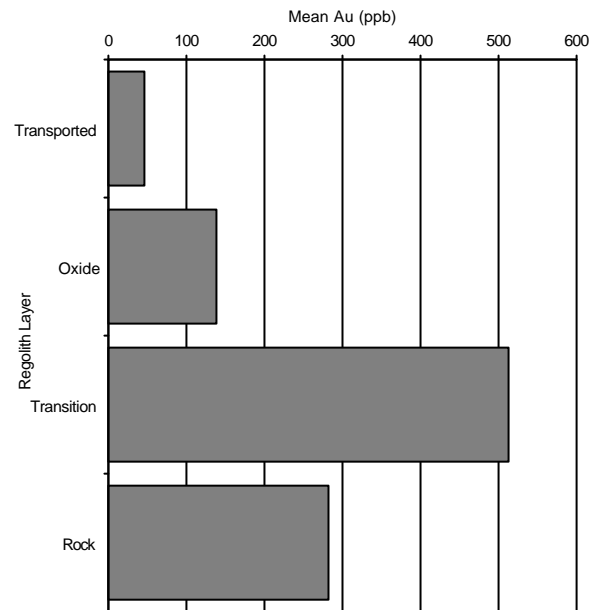


Figure 19: Mean Au concentration for each regolith layer, Federal orebody.

Calculations of mean Au contents in the regolith as a function of elevation are based on 3 m thick horizontal slices (Figure 20). The reliability of the results of each slice has been estimated using the method described in Section 2.2. Only the data for the slices considered $\geq 55\%$ reliable are interpreted. The Au concentration in the primary rock is relatively homogenous, ranging from 250 to 290 ppb. Above the weathering front, Au content increases sharply at about 300 mRL, peaking to 790 ppb about 310 mRL. It then decreases sharply upwards, returning to the bedrock abundance at 321 mRL. The gold concentration then increases slightly at the transition/oxide zone boundary (BOCO), with a substantial drop to 30 ppb in the overlying oxide zone (340-350 mRL).

Calculations of the mean Au concentration for 3 m slices as a function of distance from the weathering front (Figure 21) show similar Au contents (240-300 ppb) in primary rocks as for the calculations based on elevation (Figure 20). However, the greatest Au concentration was 660 ppb, 10 m above the weathering front, compared with the 790 ppb maximum in the elevation calculation. This suggests that Au enrichment is more dependent on elevation than distance from the weathering front. The Au-rich zone is up to 27 m thick (297-318 mRL), located directly above from weathering front, with the maximum 6-12 m above it. Compared to the primary rock, Au concentrations are 1.9-2.8-fold greater in the enrichment. Assuming that the residual Au concentration in saprolite is generally less than 1.5 times, the data suggest a chemogenic redistribution of Au from the upper regolith.

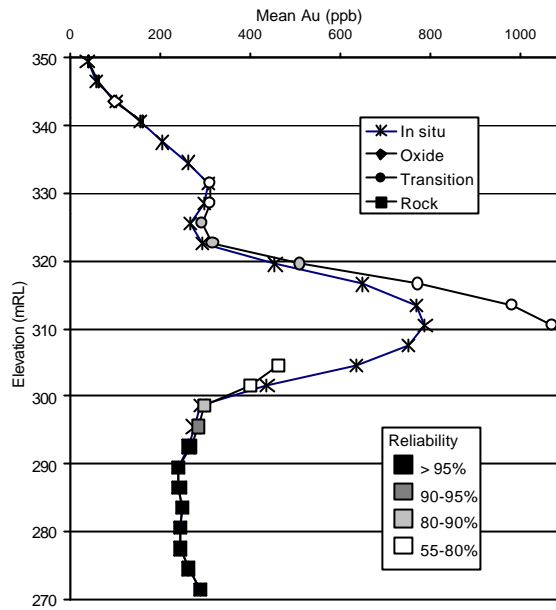


Figure 20: Mean Au concentration vs. elevation, Federal orebody.

Calculations of mean Au concentration as a function of distance from the BOCO (Figure 22) show a minor Au peak (up to 266 ppb) approximately 6 m below the BOCO. Above the BOCO, Au values decrease to 105 ppb, indicating depletion.

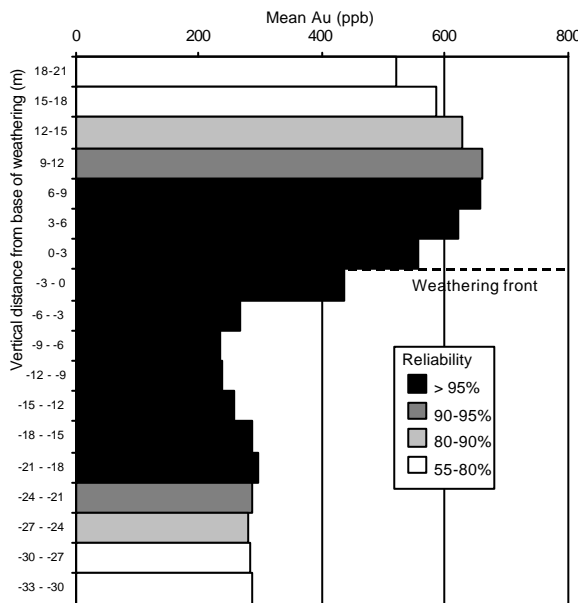


Figure 21: Mean Au concentration vs. distance from the weathering front, Federal orebody.

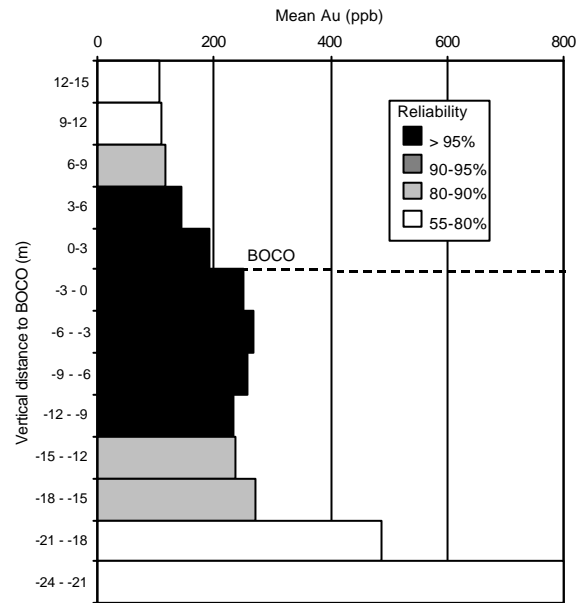


Figure 22: Mean Au concentration vs. distance from the transition/oxide zone boundary (BOCO) for the oxide and transition zones, Federal orebody.

4.1.3 Gold associations in residuum

Geochemical Au associations in the regolith were studied using cluster analysis of the multi-element data set for three drill holes (Appendix 3, Table A3.1). After testing the data variability, 23 elements were selected for further analysis, with data on Au, Br and Cl being log-transformed. Cluster analysis was performed using Ward's method as the linkage rule, with the Pearson correlation coefficient as the distance measure. Three data sets on primary rock, clay saprolite and saprolith (saprolite + saprock) were analysed with results shown as tree diagrams in Figure 23 - Figure 25.

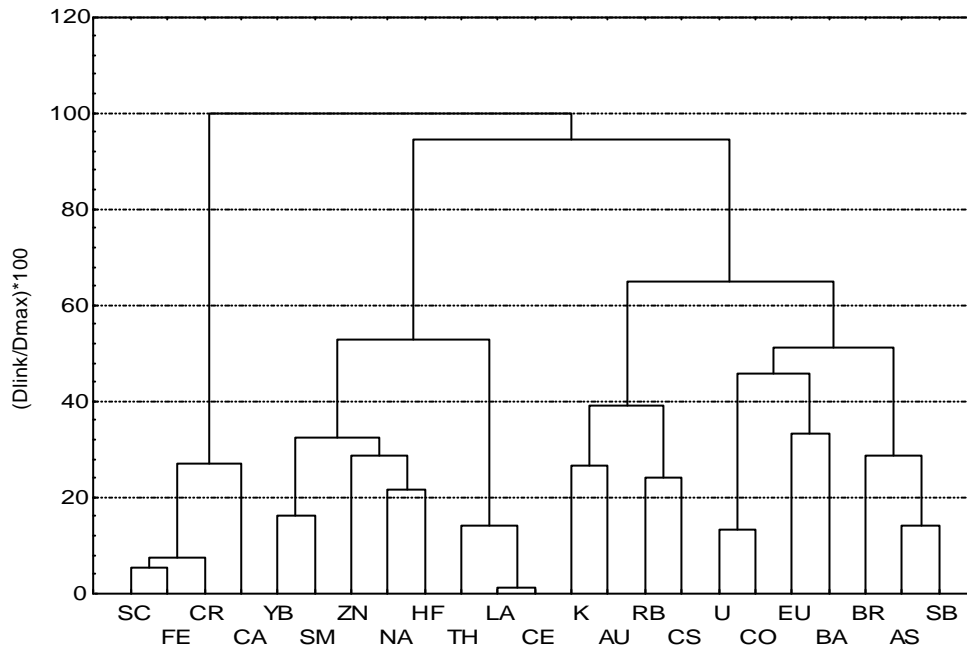


Figure 23: Associations of elements within the primary rock, Federal

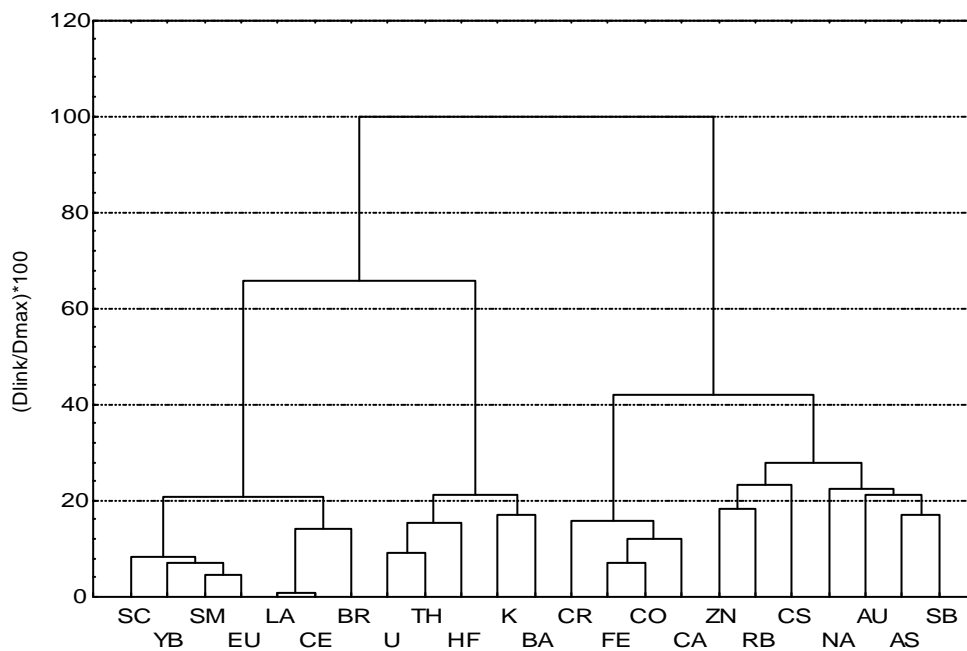


Figure 24: Associations of elements within the saprock and saprolite, Federal

In primary rock, cluster analysis of 23 variables shows that Au is associated with K, Rb and Cs, reflecting a mineral assemblage of gold and muscovite in the mineralization (Figure 23). Gold associated with primary mineralization (grouped with Na, As and Sb) is mostly retained in the saprolite (Figure 24). In the Au-depleted clay saprolite, Au is associated with Ba and Cr, reflecting residual occurrence in the upper parts of the regolith profile (Figure 25).

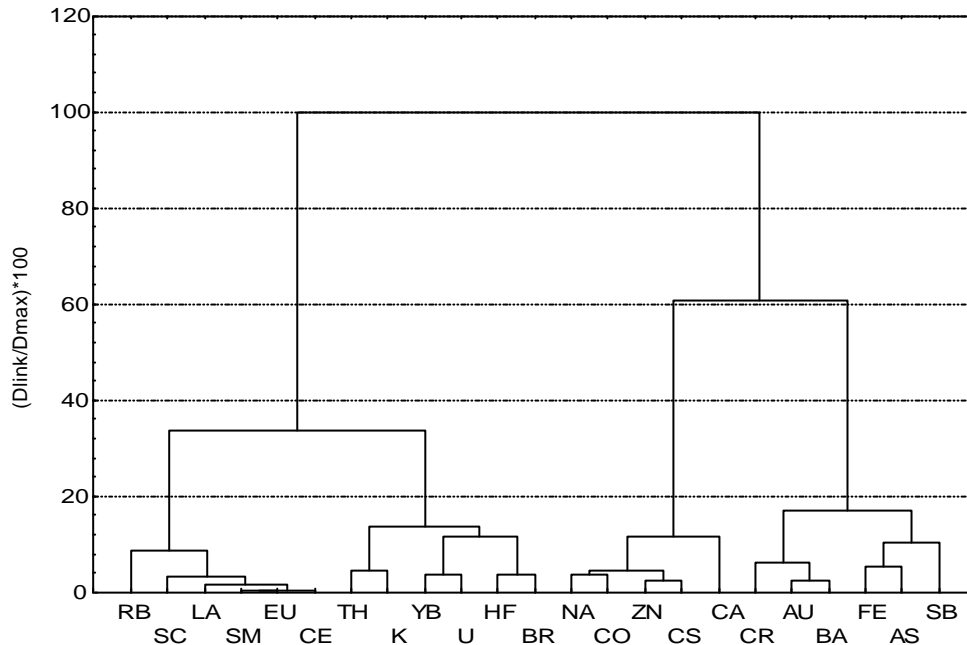


Figure 25: Associations of elements within the clay saprolite, Federal.

4.2 Gold in the transported overburden

4.2.1 Gold distribution in the transported overburden

Gold concentrations in the transported overburden are generally lower than those in the residual regolith. Local surface anomalies with Au abundances up to 200 ppb can be seen in 3D images as small spots along the mineralized structure (Figure 17). With the cut-off lowered to 90 ppb, some vertical “roots” of the surface anomalies appear, tracing through transported overburden to the residual clay saprolite. A broad patchy dispersion halo occurs at the surface up to 600 m to the NE of the orebody at a 30 ppb cut-off.

Gold concentrations are low in the silicified colluvium (19 ppb geometric mean) and hardpanized colluvium (15 ppb geometric mean) and higher in the soil (29 ppb geometric mean) and duricrust colluvium (75 ppb geometric mean).

In vertical profiles through transported overburden, Au shows significant correlation with Ca and Sr in the upper calcareous part and with Fe and As at the sediment base in the duricrust colluvium (Figure 26). In soil, hardpanized and silicified colluvium Au shows highly significant (99.9% significance level), positive correlations with Ca (0.70), Sr (0.68), Mg (0.65), S (0.63), La (0.50), Y (0.49) and Na (0.48) and negative correlations with Sc (-0.56), Al (-0.54), Si (-0.51), Ga (-0.48) and Cr (-0.44) (Appendix 4, Table 4.7). These data correspond with results of the cluster analysis that show Au to be associated with Mg, Ca, S and Sr (Appendix 4, Figure 4.2).

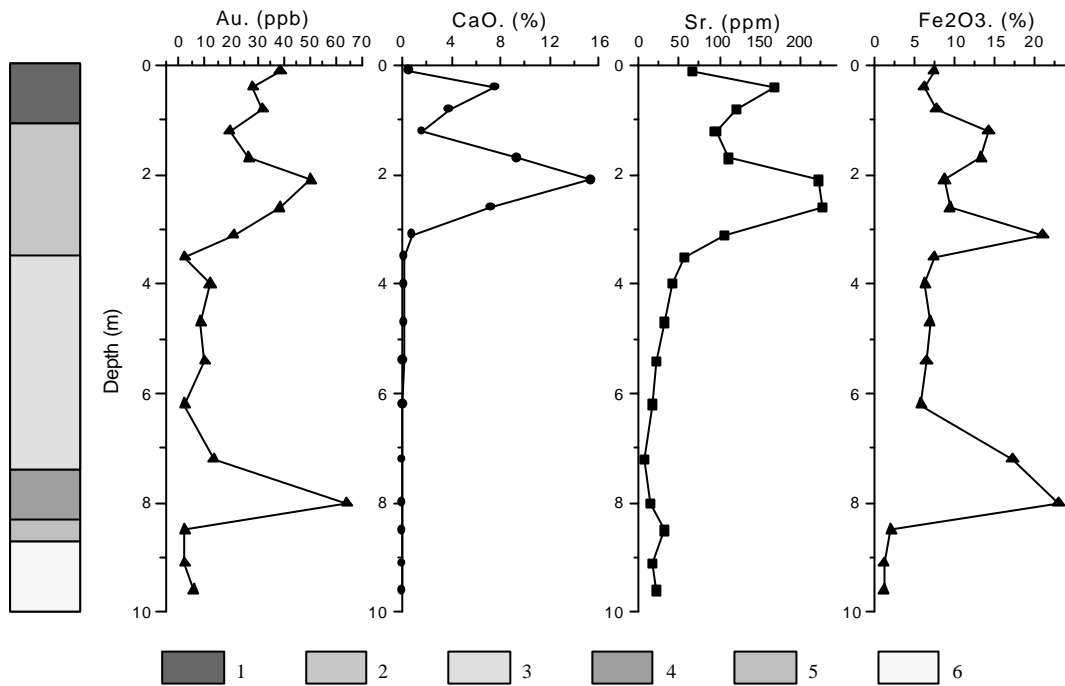


Figure 26: Distribution of Au, Ca, Sr and Fe with depth through transported overburden, NE wall of the Federal pit. Key: 1 – soil, 2 – hardpanised colluvium, 3 – silicified colluvium, 4 - duricrust colluvium, 5 – silicified clay saprolite, 6 – clay saprolite.

4.2.2 Gold concentration calculations

Calculations of mean Au concentration for the major units (Figure 19) show that the transported overburden is low in Au (45 ppb for the orebody) compared to the regolith and bedrock. Calculations of mean Au for 3 m slices as a function of distance away from the unconformity (Figure 27) show a gradual decrease through the unconformity upwards, with 56 ppb Au at the transition, decreasing to 35 ppb Au at the top. Calculations of mean Au concentration in transported material a function of distance from the surface (Figure 28) show slightly higher Au values (46 ppb) in the top 3 m.

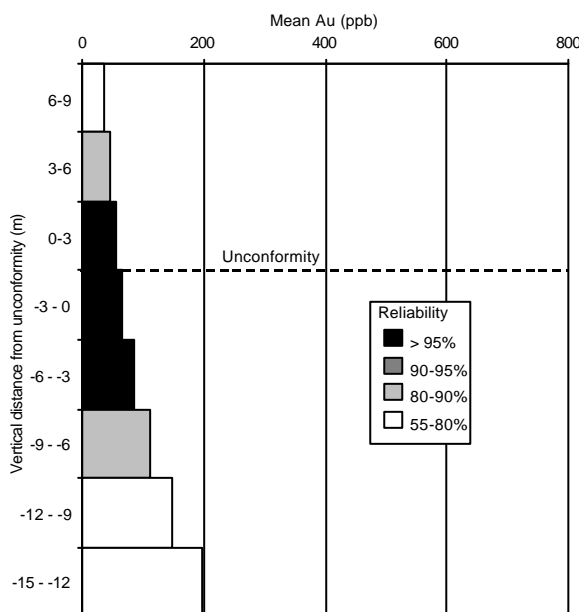


Figure 27: Mean Au concentration vs. distance from the unconformity for alluvium and oxide, Federal orebody.

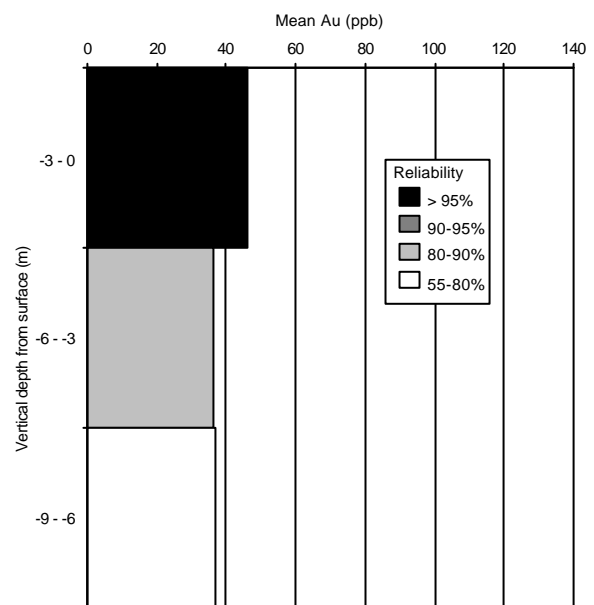


Figure 28: Mean Au concentration vs. distance from the surface for alluvium, Federal orebody.

4.2.3 Gold mass balance in transported overburden.

Seven samples of calcareous soil and sediments, and two samples of the duricrust colluvium from two Au-rich vertical profiles were separated into major fractions, namely carbonate nodules, Fe oxide nodules and quartz fragments, and analysed by XRF and INAA for major and trace elements, including Au. Bulk chemical analyses (Appendix 4, Table A4.1) were used to calculate proportions of the fraction percentage using chemical and mineral compositions of the fractions. Firstly, it was assumed that all Ca and Mg occurs as calcite and dolomite within carbonates; other elements were also included as per their concentrations in the carbonate nodules (see above). Secondly, it was assumed that all remaining Fe occurs within the Fe oxide nodules, along with other elements as per analyses of Fe oxide nodules. The remaining Si (after calculating and subtracting of Si percentage as kaolinite) was assumed to occur as quartz.

Carbonate nodule samples were crushed by hand and treated with pH 5 acetic acid for several weeks until the carbonate was completely dissolved. The solution was analysed for Au by INAA to obtain data on Au solubility. The residues were separated using a micropanner (see Section 2.1.4). Recovered Au grains were studied using an optical microscope and SEM.

The carbonate nodules, Fe oxide nodules and quartz fragments together comprise the major part of the sediments, ranging from 74 to 86% in total mass (Table 1). Carbonate nodules comprise 56-70% of total mass in soil and colluvium but only account for 31% in the duricrust colluvium (6-7 m depth) in profile 1. In profile 2, the proportion of the carbonate nodules decreased to 21-39%, with a substantial percentage (15-25%) of Fe oxide nodules. Duricrust colluvium has 51% of Fe oxide nodules.

Mineral compositions of the carbonate nodules, calculated using SOILS.MH software (M.Hart, CSIRO) show that they consist of calcite with kaolinite and silica. Dolomite, Fe oxides, muscovite and albite occur as minor minerals (Table 2).

Data on Au demonstrate some differences between two profiles studied (Table 1). The carbonate nodules have Au concentrations ranging 180-380 ppb in profile 1 and 70-90 ppb in profile 2. The Fe oxide nodules have more variable compositions, ranging from 48 to 410 ppb in profile 1, with maximum concentration (410 ppb) at 3-5 m depth, and from below detection (5 ppb) for nodules in soil and colluvium to 91 ppb in duricrust colluvium in profile 2. Similar results are observed for quartz fragments: Au abundances range from 9-40 ppb in profile 1 and are below detection in profile 2, except for the duricrust colluvium which contains 106 ppb Au. These data indicate various sources for both quartz and Fe oxide materials in the transported overburden.

Gold mass balance calculations show that carbonate nodules contain the greatest (83-97%) proportion of total Au, despite the high Au concentrations in some of the Fe oxide nodules. Proportions of Au in Fe oxide nodules ranged from 1 to 12% in colluvium and show higher proportions (17-65%) in duricrust colluvium (samples 431/7 and F115). Quartz contained negligible proportions of Au, except for the duricrust colluvium sample F115, in which 35% of the Au is in quartz.

Table 1: Gold mass balance in major fractions of transported overburden, Federal.

Profile	Depth (m)	Zone	Sample #	Fraction	Weight (% of total)	Au content (ppb)	Au mass (% of total)
1	2-3	HC	431/3	Carbonate nodules	62	181	97
				Fe oxide nodules	5	53	2
				Quartz	14	9	1
1	3-4	HC	431/4	Carbonate nodules	67	305	91
				Fe oxide nodules	5	349	8
				Quartz	10	14	1
1	4-5	HC	431/5	Carbonate nodules	70	352	88
				Fe oxide nodules	7	410	11
				Quartz	9	40	1
1	5-6	HC	431/6	Carbonate nodules	56	327	87
				Fe oxide nodules	20	127	12
				Quartz	10	25	1
1	6-7	DC	431/7	Carbonate nodules	31	382	83
				Fe oxide nodules	51	48	17
				Quartz	2	14	0
2	4-5	HC	F15	Carbonate nodules	21	93	93
				Fe oxide nodules	25	<5	3
				Quartz	30	<5	4
2	5-6	HC	F16	Carbonate nodules	32	87	93
				Fe oxide nodules	15	<5	1
				Quartz	28	6	5
2	6-7	HC	F17	Carbonate nodules	39	68	97
				Fe oxide nodules	15	<5	1
				Quartz	23	<5	2
2	14-15	DC	F115	Carbonate nodules	-	-	0
				Fe oxide nodules	51	91	65
				Quartz	23	106	35

Zones: HC – hardpanized colluvium, DC – duricrust colluvium.

- Sample numbers as referred to in Appendix 4

Table 2: Calculated mineral compositions of carbonate nodules, Federal.

Profile	Depth (m)	Calcite (%)	Dolomite (%)	Kaolinite (%)	Muscovite (%)	Albite (%)	Goethite (%)	Quartz (%)	Anatase (%)	Total (%)
1	2-3	56.1	3.3	13.1	3.0	1.6	3.1	13.7	0.2	94.0
1	3-4	46.6	5.1	14.1	3.6	3.1	4.2	19.8	0.3	96.7
1	4-5	60.4	5.5	10.4	2.5	2.1	3.1	12.9	0.2	97.1
1	5-6	60.7	7.3	10.6	2.3	1.8	2.1	11.8	0.2	96.8
1	6-7	51.4	15.9	11.5	2.0	1.7	2.3	12.4	0.2	97.4
2	4-5	77.2	2.5	6.5	0.9	0.5	2.0	8.5	0.1	98.1
2	5-6	81.4	3.1	4.9	0.9	0.5	1.2	5.1	0.1	97.1
2	6-7	29.3	2.9	23.5	4.1	4.8	5.7	23.6	0.3	94.2

To separate particulate Au from carbonate nodules, eight samples were treated with pH 5 acetic acid until the carbonate minerals were completely dissolved. The solution and residue were analysed for Au by INAA, with results shown in Table 3. Substantial (34-82%) proportions of the samples were dissolved, and are in good agreement with the calculated percentage of carbonate minerals (Table 2). The solutions contain 12-83 ppb dissolved Au. Mass balance calculations indicate that a substantial

amount (8-29%) of Au was dissolved. This indicates that, in part, Au occurs as a mobile element in calcareous materials. The results on particulate Au, discussed below in Section 5.2.3, and strong correlations of Au with Ca, Mg and Sr support these suggestions.

Table 3: Gold concentrations and mass balance for experiments on carbonate dissolution.

Profile	Depth (m)	Total weight (g)	Residue weight (g)	Dissolved material (%)	Calculated carbonates (%)	Total Au content (ppb)	Total Au mass (mg)	Au content in solution (ppb)	Au mass in solution (mg)	Dissolved Au (% of total)
1	2-3	84.2	32.0	62.0	59.4	181.0	15232	42.7	3590	23.6
1	3-4	168.4	81.2	51.7	51.7	305.0	51354	83.1	14000	27.3
1	4-5	228.8	98.9	56.8	65.9	352.0	80544	27.6	6320	7.8
1	5-6	132.4	41.7	68.5	68.0	327.0	43286	50.7	6710	15.5
1	6-7	37.7	11.5	69.4	67.3	382.0	14401	26.3	993	6.9
2	4-5	56.6	10.0	82.3	79.7	92.6	5244	26.5	1500	28.6
2	5-6	97.4	12.2	87.5	84.5	86.5	8425	16.7	1630	19.3
2	6-7	156.9	103.1	34.3	32.2	68.4	10731	12.0	1890	17.6

5 CHARACTERISTICS OF PARTICULATE GOLD AT FEDERAL

5.1 Introduction

Gold grains were extracted from two bulk (5-10 kg) samples taken from the northern part of the open pit, and from five 1-2 kg samples from drill cuttings (Table 4), representing Au-rich saprolite, saprock and primary mineralization. The samples were separated using techniques described in Section 2.1.4. The results of the Au grain study are discussed below and photos of the Au grains enclosed in Appendix 1, Plates A1.1-A1.3.

Table 4: Gold concentration in the bulk samples

Regolith zone	Sample location	Depth (m)	Gold grade (ppm)
Saprolite	WCUCD 411	38-39	0.13
	WCUCD 436	63-64	1.12
Saprock	WCUCD 431	79-80	0.46
Primary mineralization	WCUCD 511	107-108	1.05
	WCUCD 431	104-105	0.39
	Open pit, F1	65	3.26
	Open pit, F14	65	74.90

5.2 Characteristics of gold grains

5.2.1 Gold in primary mineralization

In the primary mineralization, Au grains are relatively small, commonly less than 100 μm in diameter, with some larger particles up to 500 μm in size. Most grains are irregular in shape and xenomorphic, with rough surfaces (Photos 3-6). Some of the surfaces are smooth, due to imprinting from adjacent minerals. The principal minerals associated with Au in primary mineralization are pyrite and aluminosilicates, usually hornblende and biotite (Photos 1-5). All primary Au grains contain approximately 5-10% Ag, according to SEM.

5.2.2 *Gold in the residual regolith*

In the saprock and the saprolite, Au grains occur as primary, slightly corroded grains containing some Ag and as high-fineness, supergene Au crystals (Photos 7-12). The supergene crystals are very small, commonly less than 20 µm in diameter. The majority are subhedral, with euhedral crystals less common. Very thin, platy pseudo-hexagonal crystals are predominant, with minor prismatic and tabular crystal forms and rounded grains. Pristine crystals are rare; most crystals have rough surfaces, pits, cavities and imprints from adjacent minerals. All supergene crystals are of high fineness and contain no Ag (at the detection limit of energy dispersion X-ray system, which ranges from 0.1 - 1.0%). In contrast to primary Au, supergene Au grains commonly have no intergrowths or inclusions of other minerals, although rarely there are inclusions of aluminosilicates (Photo 10).

5.2.3 *Gold in carbonate materials*

Particulate Au was separated from 8 samples of carbonate nodules using the residues after carbonate dissolution (see Chapter 4.2.3). Gold grains were found in two samples: 13 grains in the sample 431/5 and 3 grains in the sample 431/6. One grain of Os-Pt composition was recovered from the sample 431/5.

All Au grains recovered are of high fineness with no Ag. Some EDX analyses of Au grains show a higher C peak compared to the normal C signal arising from the glue used for sample preparation, but it is difficult to distinguish a useful signal and different sample preparation technique is needed. The Au grains are of different morphologies, varying from xenomorphic oval and platy grains to pristine crystals. Some of the particles are strongly corroded (Photo 13) possibly as a result of the acid pre-treatment. Two Au morphologies are different from the supergene Au found in the regolith: thin platy particles (Photos 14-15) and complex aggregates (Photos 16-18). Unlike the supergene crystals in the regolith, platy particles in the carbonate nodules have no definite crystal shapes, and their surfaces show hatching (Photo 14). Complex aggregates mainly consist of very fine (1-6 µm) oval, spheroidal and slightly crystallised particles connected together directly or by rods (Photos 17-18). Some of the larger grains consist of agglomerated small micrometre-size particles. These Au aggregates contain traces of Fe and Ti, but no Ag.

5.3 Discussion

Particulate Au at Federal shows similar characteristics to that in many other sites in the Yilgarn Craton (*e.g.*, Freyssinet and Butt, 1988; Gedeon and Butt, 1990; Lawrance and Griffin, 1994; Porto *et al.*, 1999, Sergeev and Gray, 1999). Primary Au grains are irregular and xenomorphic and alloyed with Ag (up to 10%). The grains are also associated with pyrite, which is typical for Au-sulphide mineralization in the Yilgarn Craton.

Unlike primary Au, supergene particulate Au occurs mainly as small crystals of high fineness with very low or no detectable Ag. At Federal, supergene Au is smaller in size than other sites, with a majority of particles less than 20 µm in diameter. The principal Au crystal forms are very thin platy, pseudo-hexagonal crystals, similar to those observed at the Panglo and Hannan South deposits.

The characteristics of the supergene Au crystals in the Yilgarn Craton do not give us direct indicators of the mechanism of Au transport in the regolith. The Au chemical composition, hydrogeochemistry and Eh-pH constraints support Au remobilization as halide complexes. Lack of specific supergene minerals in association with supergene Au indirectly supports this hypothesis because halides (mostly halite) are highly soluble in water (used for Au grain separation). The dependence of the supergene Au crystal shape on transport conditions, *e.g.*, groundwater salinity, is still unclear and needs more data.

Gold grains found in carbonate nodules are different in shape from those in the primary mineralization and the regolith. Fragile, complex Au aggregates, to some extent, resemble those found in some of the Alaskan and South Australian placers, that are interpreted as Au-replaced bacteria (Watterson, 1992; Keeling, 1993). The possibility of a bacterioform origin of these Au particles needs further investigation.

6 HYDROGEOCHEMISTRY

6.1 Introduction

The primary justification given for the use of hydrogeochemistry in mineral exploration is that groundwater anomalies may be broader and more regular than the primary mineralization and the secondary dispersion haloes in the regolith, thus enhancing the geochemical signature. In addition, areas of high chemical reactivity (*e.g.*, faults and shear zones) may have distinct hydrogeochemical signatures even where the “solids” are unremarkable in terms of elemental abundances, and where petrographic study is difficult. Hydrogeochemical studies also provide information on how various materials are weathering. This enhances understanding of active dispersion processes and assists in the development of weathering and geochemical models that are essential for effective exploration in regolith-dominated terrain.

Therefore, the aims of this hydrogeochemical study were:

- (i) to yield data on geochemical dispersion processes, and to assist in interpretation of geochemical data;
- (ii) to provide information on whether groundwater can be used successfully as an exploration medium in this area in particular and, in conjunction with other studies, in the central Yilgarn in general;
- (iii) to check for differences in groundwaters contacting granitic rocks in comparison with other Archean rock types;
- (iv) to contribute to a groundwater database on the characteristics of groundwaters at various sites, and to enhance our understanding of groundwater processes in mineralized zones.

6.2 Compilation of results and comparison with other sites

The concentrations of various ions at Woodcutters and at other sites are plotted versus salinity (TDS) or pH in Appendix 5, Figures A5.1 – A5.36. The sea water data (Weast *et al.*, 1984) are used to derive the line of possible values (denoted as the sea water line) if sea water (TDS 3.5%) were diluted with freshwater or concentrated by evaporation; the line is shown on each figure except where the concentration in sea water is too low to be observable, relative to the concentration of the element in groundwaters. The results from Woodcutters can be compared with those from other sites in southern WA, which are grouped as follows:

- (i) *Northern groundwaters* (Northern Yilgarn and margins) - Lawlers (Gray, 1994) and Baxter (Gray, 1995). Groundwaters in these areas are fresh and neutral, trending more saline in the valley floors.
- (ii) *Central groundwaters* (close to and north of the Menzies line) - Granny Smith (Gray 1993a), Golden Delicious (Bristow *et al.*, 1996), Mt. Gibson (Gray, 1991) and Boags (Gray, 1992a)
Groundwaters are neutral and brackish (commonly < 1% TDS) to saline (about 3% TDS), trending to hypersaline (10 - 30% TDS) at the salt lakes, with common increases in salinity with depth.

(iii) *Kalgoorlie groundwaters* -

Golden Hope mine, (Gray, 1993b), Wollubar palaeochannel (Gray, 1993b), Panglo deposit (Gray, 1990), Baseline mine, Mulgarrrie palaeochannel (Gray, 1992b), Steinway palaeochannel (Lintern and Gray, 1995a) and Argo palaeochannel (Lintern and Gray, 1995b).

These groundwaters are commonly acid (pH 3 - 5), except where buffered by extremely alkaline materials (*e.g.*, ultramafic rocks), and saline within the top part of the groundwater mass, trending to more neutral (pH 5 - 7) and hypersaline at depth and where within a few kilometres of salt lakes.

(iv) *Officer Basin* - Mulga Rock palaeodrainage system (Douglas *et al.*, 1993).

Groundwaters are saline to hypersaline and neutral to acid. The major ion chemistry is similar to that of the Kalgoorlie region, but the dissolved concentration of many other ions is low, due to sorption on lignites in the channel sediments.

Wollubar, Baseline and Panglo are acid groundwater systems, whereas the other sites have dominantly neutral groundwater. Comparisons with other sites may be useful in indicating the significance of any particular element anomaly, and whether the groundwater composition is affected by particular lithological interactions. Specific descriptions of the varying sites are found in the referenced reports, with generalized descriptions of the hydrogeochemistry of the Yilgarn Craton given in Gray (1996) and Butt *et al.* (1997).

Saturation index (SI) values for various minerals (Section 2.1.5) are plotted in Appendix 6, Figures A6.1 – A6.28. The equilibrium point is shown as a dashed line. The shaded area denotes the zone in which waters may be in equilibrium with that mineral. Note that where a mineral has a very broad zone, this indicates significant uncertainty in the thermodynamic data for this mineral and/or calculation problems - *i.e.*, samples within that zone are not necessarily at equilibrium, though samples above or below the zone are out of equilibrium. In addition, the distributions of elemental concentrations are plotted in Appendix 7, Figures A7.1 – A7.30.

6.3 Acidity and oxidation potential

An Eh-pH plot of waters from Woodcutters and other sites is shown in Figure 29, along with the particular redox couples controlling groundwater Eh and pH, namely:

Fe - controlled by redox reactions between dissolved Fe²⁺ and Fe oxides

Mn - controlled by redox reactions between dissolved Mn²⁺ and Mn oxides

Al - controlled by reactions between dissolved Al³⁺ and kaolinite and other aluminosilicates.

These redox couples are described in detail in Gray (1996). Groundwaters are combined into the various groups, as described in Section 6.2. The Woodcutters groundwaters are neutral in the Grand and Criterion areas, tending to acid (pH 5.8) in the Federal area. Also included in Figure 29 is the minimum Eh required for dissolution of 0.2 ppb Au in Cl and/or iodide enriched groundwaters: none of the groundwaters have Eh values high enough to allow dissolution of >0.2 µg/L Au. As described below (Section 6.6), this is entirely consistent with the observed dissolved Au concentrations.

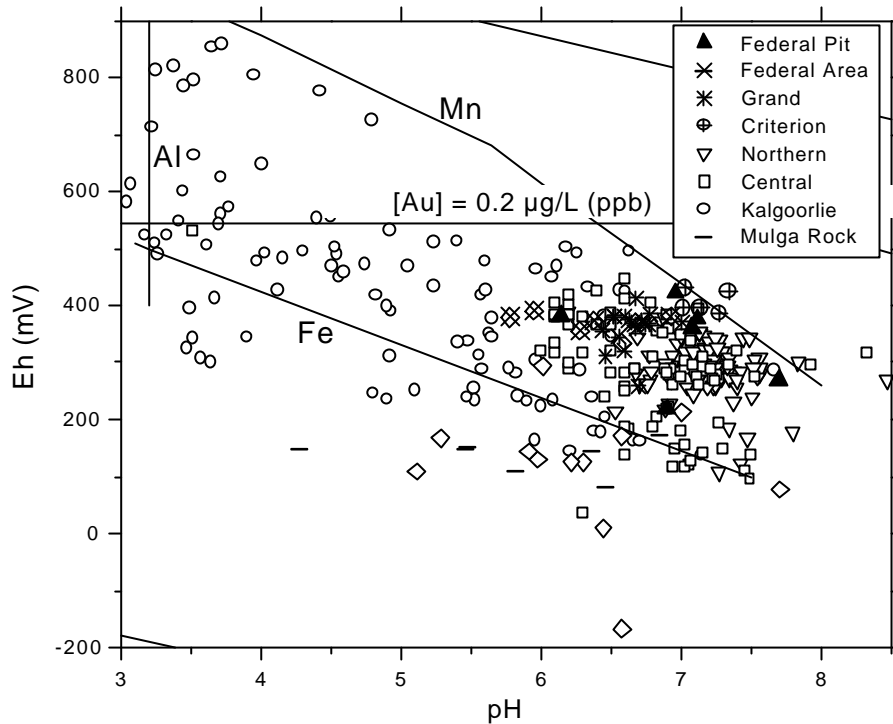


Figure 29: Eh vs. pH for groundwaters from Woodcutters and other sites. Key: Fe - $Fe^{2+}/Fe(OH)_3$, Al - $Al^{3+}/kaolinite$, Mn - Mn^{2+}/Mn_xO_y ,

6.4 Salinity effects and major element hydrogeochemistry

Data are plotted in Appendix 5, Figures A5.1 – A5.14. The Woodcutters groundwaters range from weakly saline at Criterion (0.4 - 1% TDS, compared with sea water salinity of 3.5% TDS) trending to higher salinities (0.8 – 2.9% at Grand and 1.0 – 6.8% for Federal) to the south. These trends in acidity and salinity (Figure 30) fit within the variations observed for Central Yilgarn groundwaters, though some of the Federal groundwaters have lower pH values than for others in this group. For most of the major elements (Na, Mg, Cl, SO_4), the element/TDS plots lie on a straight line defined by that for dilution or concentration of sea water (Figures A5.1, A5.3, A5.5 and A5.6). This implies that these groundwaters are in some manner (*e.g.*, by previous sea water incursion or from salt aerosol) sourced from sea water and then subsequently concentrated by evaporation. The Grand and Criterion groundwaters are moderately depleted in K, relative to the concentrations expected if the groundwater had been diluted sea water (Figure A5.2, shown in more detail in Figure 31), whereas the Federal groundwaters show a significant K depletion, a characteristic commonly observed for Kalgoorlie groundwaters which is probably due to precipitation of alunite [$KAl_3(SO_4)_2(OH)_6$] in acid groundwater systems, as a by-product of the dissolution of kaolinite and other aluminosilicates (Gray, 1996). Thus the pH and major element data suggest the groundwaters at Woodcutters to trend from “Central-type” in the north towards “Kalgoorlie-type” at Federal.

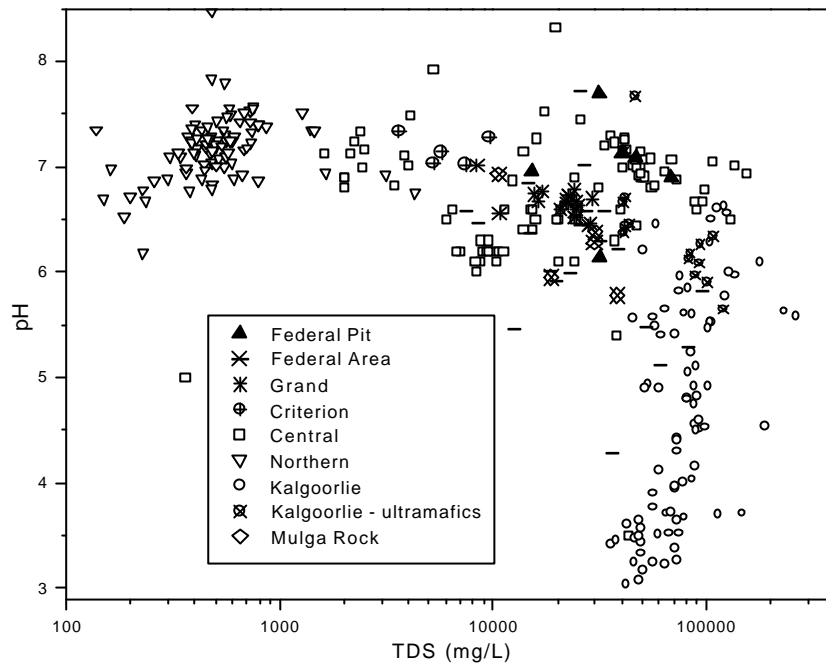


Figure 30: pH vs. TDS for groundwaters from Woodcutters and other sites

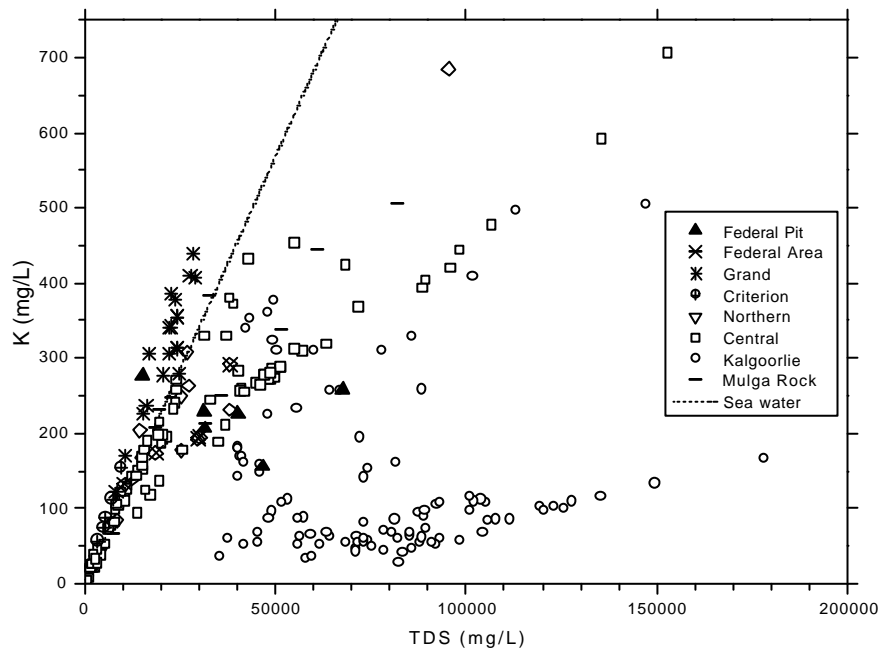


Figure 31: Potassium vs. TDS for groundwaters from Woodcutters and other sites

The groundwaters at Woodcutters have salinities well below that required for halite saturation (Figure A6.1), although the most saline samples are close to equilibrium with gypsum (Figure A6.2) and celestine (Figure A6.3), reflecting the relatively high Sr proportions at Woodcutters (Figure A5.7). Other major elements that appear to be controlled by equilibration with respect to a number of minerals in some or all of the groundwaters are Ca (calcite; Figure A6.5), Mg (sepiolite, dolomite and/or magnesite; Figures A6.6, A6.7 and A6.9), Ba (barite; Figure A6.4), Si (amorphous silica and/or sepiolite; Figures A6.8 and Figure A6.9), Mn (rhodochrosite; Figure A6.15) and Al (amorphous alumina; Figure A6.13).

6.5 Minor element hydrogeochemistry

Concentrations of the minor elements (Table 5; Figures A5.15 – A5.36) show similar trends to the major element and acidity data. The Grand and Criterion groundwaters are comparable to Central groundwaters, whereas the Federal groundwaters trend towards a Kalgoorlie-type groundwater. In particular, Li, base metals, Ag and Au (Figures A5.10, A5.19 – A5.24, A5.27 and A5.34), have greater concentrations in the Federal groundwaters, than at Grand or Criterion.

Table 5: Median minor element compositions of groundwaters.

	Woodcutters samples				Northern	Central	Kalgoorlie	Mulga Rock	Sea water	Controls
	Federal Pit (6)	Federal Area (5)	Grand (19)	Criterion (5)						
Li	0.208	0.225	0.040	0.025	<0.005	<0.005	0.9	nd	0.18	Ac ?
Ba	0.033	0.070	0.025	0.050	0.04	0.02	0.04	0.03	0.013	Eq/Min
Sc	< 0.005	< 0.005	< 0.005	< 0.005	0.009	0.017	0.019	nd	0.0000006	Ac/Min
V	< 0.005	< 0.005	< 0.005	0.005	0.007	<0.005	<0.005	nd	0.002	?
Cr	0.04	0.04	0.04	0.03	0.01	<0.005	0.003	0.002	0.0003	Um
Mn	0.73	0.08	0.12	0.07	0.01	0.1	2	0.3	0.0002	Mf/Um/Ac
Fe	0.19	0.20	0.20	0.21	0.003	0.05	0.1	1	0.002	S
Co	0.026	0.009	0.005	0.002	<0.0005	0.002	0.16	<0.002	0.00002	Um/Mf/Ac
Ni	0.100	0.090	0.060	0.050	0.002	0.001	0.26	0.020	0.00056	Ac/Mf/Um
Cu	0.008	0.010	0.005	0.003	0.003	0.003	0.05	0.00	0.00025	Ac/Mf
Zn	0.050	0.030	0.025	0.015	0.006	0.01	0.05	0.04	0.0049	Ac/Mf
Ga	< 0.001	< 0.001	< 0.001	< 0.001	0.002	<0.005	0.006	nd	0.00003	S
As	< 0.01	< 0.01	< 0.01	< 0.01	<0.0002	0.09	<0.02	<0.02	0.0037	S
Mo	0.010	< 0.002	0.002	< 0.002	0.001	0.009	<0.01	nd	0.01	S
Ag	0.0014	0.0029	< 0.0001	< 0.0001	<0.001	0.0005	0.001	nd	0.00004	?
Cd	< 0.005	< 0.005	< 0.005	< 0.005	<0.002	0.001	<0.002	<0.001	0.00011	?
Sb	< 0.002	< 0.002	< 0.002	< 0.002	<0.0003	0.001	<0.001	<0.0004	0.00024	S
REE	<0.002	<0.002	<0.002	<0.002	<0.002	<0.008	0.8	0.013	0.000013	Ac
W	0.006	0.010	0.010	< 0.005	<0.0002	0.001	0.001	nd	0.0001	S
Au	0.028	0.065	0.006	0.005	0.004	0.03	0.05	0.001	0.004	Min
Pb	0.01	< 0.01	< 0.01	< 0.01	<0.001	0.001	0.06	0.012	0.00003	Ac/Min
Bi	< 0.001	< 0.001	< 0.001	< 0.001	<0.0002	0.001	<0.001	<0.002	0.00002	S ?

All concentrations in mg/L (ppm), except Au in µg/L (ppb)

nd: not determined

Number of samples given in brackets

Eq mineral equilibrium

Ac enriched in acid groundwaters

Um enriched in waters contacting ultramafic rocks

Mf enriched in waters contacting mafic rocks

Min enriched in waters contacting Au mineralization

S enriched in waters contacting weathering sulphides

Sal enriched in saline groundwaters

? not clearly defined

6.6 Gold chemistry

The moderate salinity of the groundwaters at this site means that the dominant mechanism for the mobilization of Au in the southern Yilgarn, namely as the chloride complex (AuCl_2^-):



is expected to be significant at Woodcutters, but at much lower Au concentrations (Figure A5.34) than in the Kalgoorlie region, due to the lower oxidation potential of these groundwaters (Section 6.3; Figure 29). The Woodcutters groundwaters are all above equilibrium for Au metal (Figure A6.29), indicating a poor capability of these groundwaters to dissolve Au, even at the small concentrations observed. In all cases (Figure 32) the groundwaters have measured oxidation potentials below that required for dissolution of $0.002 \mu\text{g/L}$ Au.

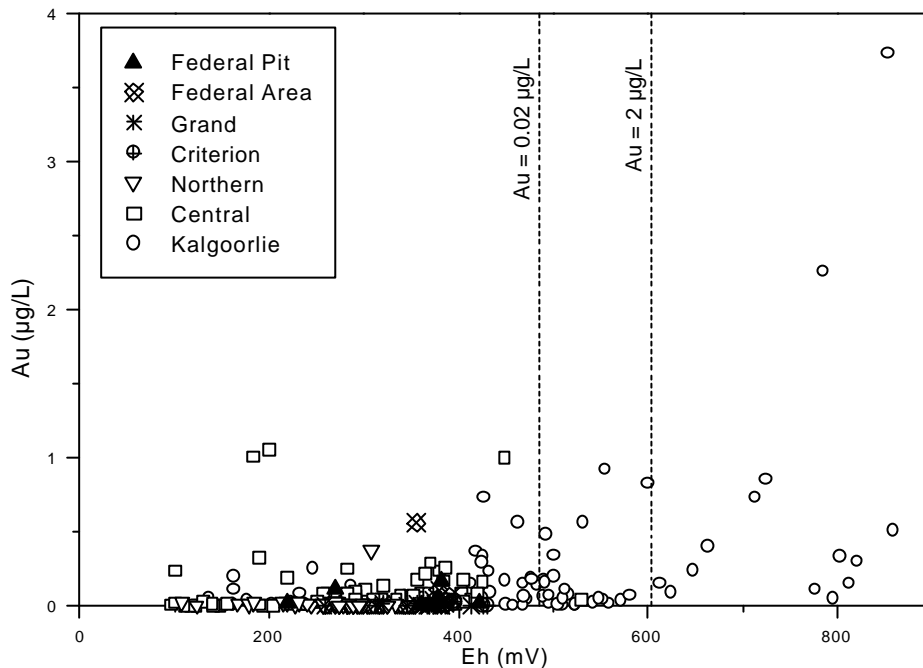


Figure 32: Dissolved Au concentration vs. Eh for Woodcutters and other Western Australian groundwaters, with the Eh values for dissolution of 0.02 and $0.2 \mu\text{g/L}$ Au.

6.7 Mapping of the groundwater data

Element distributions of Woodcutters groundwaters are given in Appendix 7, Figures A7.1 - A4.30. The most clearly observed feature is the lower pH values (Figure A7.4) and greater concentrations of Au (Figure 33), Li, Mn, Co, Ni, Cu, Zn, Ag, Y and REE (Figures A7.2, A7.9 – A7.14, A7.19, A7.20 – A7.22) in the Federal groundwaters, relative to those at Grand and Criterion. As a result of this effect and the small number of “background” samples, no clear hydrogeochemical signature could be derived that mirrored the presence of mineralization in the Woodcutters area. The best candidate as a hydrogeochemical pathfinder for Au in this area (particularly considering results from elsewhere; Gray, 1996) is Mo (Figure 34), though results are equivocal, possibly because of a lack of background samples.

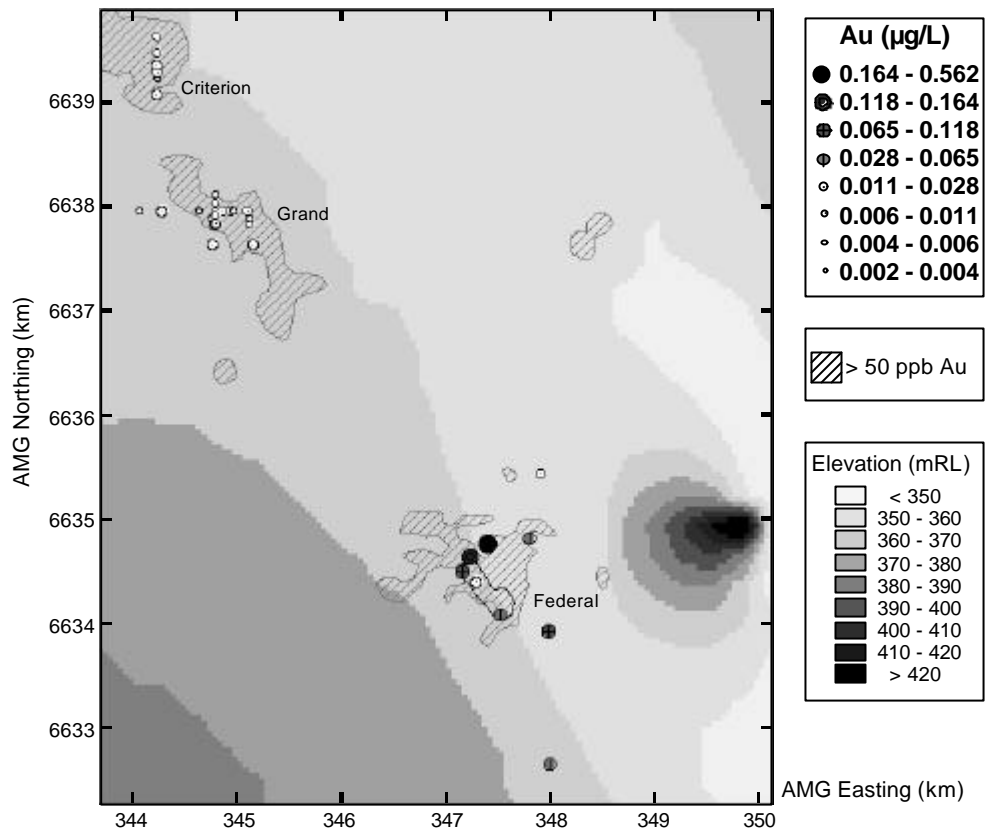


Figure 33: Dissolved Au distribution at Woodcutters, with the areas where average Au grades are greater than 50 ppb, the Federal Pit and the surface elevation also shown.

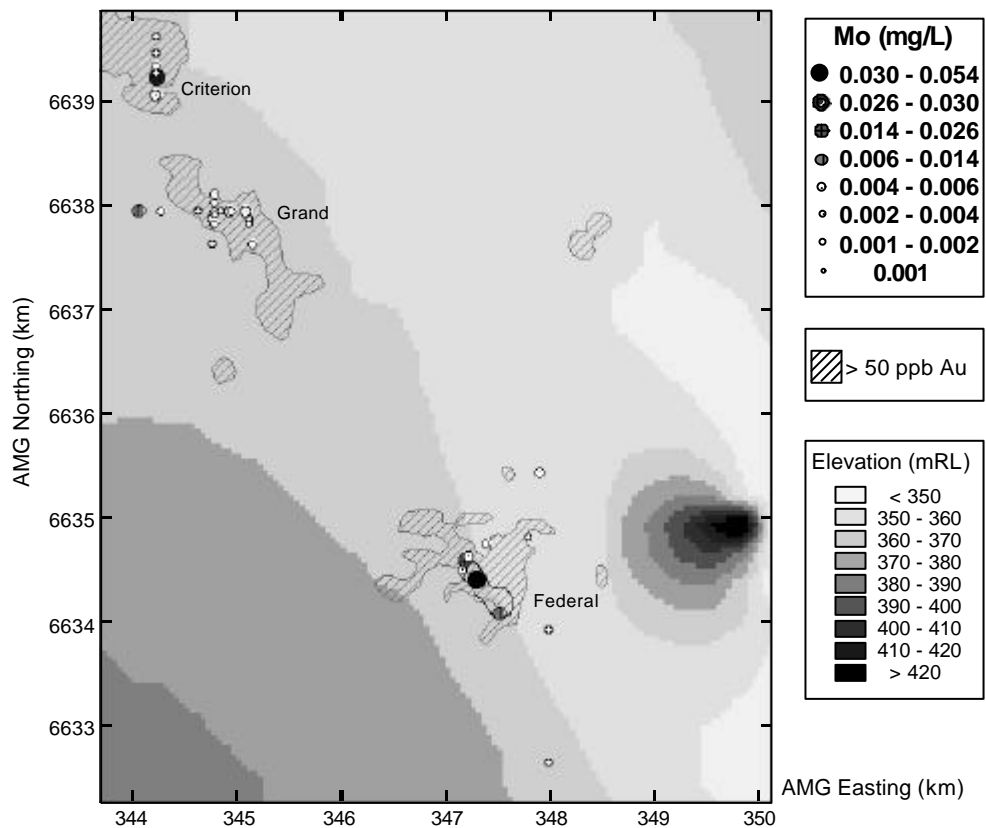


Figure 34: Dissolved Mo distribution at Woodcutters, with the areas where average Au grades are greater than 50 ppb, the Federal Pit and the surface elevation also shown.

7 CONCLUSIONS

7.1 Regolith and landform evolution

For an extended period prior to the Eocene, warm and humid climate conditions and stable landscape favoured weathering in the Yilgarn Craton (Mabbutt, 1980). In the Woodcutters area, granitoids of the Scotia pluton are deeply weathered (up to 60 m), with weathering extending a further 5-25 m over the Federal mineralized zone due to sulphide weathering. The specific hornblende-rich composition of granodiorites and monzogranites in the area led to development of smectite in the saprolite. The uppermost, bleached clay saprolite is overlain by a continuous 2-16 m thick cover of transported duricrust pisoliths, mostly derived from granite terrain (Mahizhnan, 2000). This indicates truncation of the residual laterite and much of the mottled zone in the area. Regolith evolution under semi-arid to arid conditions since the Miocene included further deposition of sediments, accompanied by silicification of the base sediment facies and top of the residual profile, and development of pedogenic carbonates close to the surface.

7.2 Gold geochemistry

At the Federal deposit, Au in the regolith is enriched at two levels (Figures 14-17): at the weathering front and at the top of the transition zone. The major supergene Au enrichment and dispersion occur at the base of the regolith as a horizon up to 27 m thick, with maximum Au concentrations 6-12 m above the weathering front. Compared to the primary rock, Au concentrations are 1.9-2.8-fold greater in the enrichment zone. Assuming that the residual Au concentration in saprolite is generally less than 1.5 times compared to primary rock, the data indicate chemogenic Au redistribution from the upper regolith. A patchy enrichment zone extends up to 400 m E, at a 60 ppb cut-off. However, much of this enrichment zone is located above the slightly (up to 30 ppb) mineralized primary rocks, suggesting that this blanket is a combination of residual and absolute enrichment.

The upper enrichment is several metres below the transition/oxide zone boundary. Within the orebody, the supergene enrichment occurs as a chain of local Au-rich (up to 1 ppm) spots along the mineralized structure, with a decreased Au concentration above the boundary due to depletion. The overlying oxide zone is Au depleted.

In the transported overburden, Au is concentrated at the base of the duricrust colluvium and near the surface in calcareous soil and colluvium. In the duricrust colluvium, Au is mostly enclosed within ferruginous nodules and quartz, indicating mechanical Au transport. In the calcareous materials, the majority of Au (83-97%) is enclosed within carbonate nodules indicating chemogenic Au mobilization in the calcrete environment. The morphology of supergene Au grains possibly suggests a bacterioform origin.

7.3 Hydrogeochemistry

Groundwaters in the Woodcutters area are neutral and less saline in the northern Grand and Criterion areas, tending to acid (pH 5.8) and saline in the Federal area. However, they are less corrosive than in the Kalgoorlie region, and none of the groundwaters have Eh values high enough to allow dissolution of appreciable Au, consistent with the low concentrations of Au dissolved in all groundwaters.

The differences in groundwater characteristics are reflected in greater Li, base metals, Ag and Au concentrations in the Federal groundwaters, relative to those at Grand or Criterion. No clear hydrogeochemical signature could be derived that mirrored the presence of mineralization in the

Woodcutters area. The best candidate as a hydrogeochemical pathfinder for Au in this area is Mo, though results are equivocal, due to a lack of background samples.

7.4 Implications for exploration

In primary mineralization at Federal the concentration of pathfinder elements (As, Sb, Ag, W, and Mo) is generally low. According to cluster analysis, Au in primary mineralization is associated with K, Rb and Cs, but use of these elements as pathfinders is doubtful because of an occurrence of various K-minerals in the regolith, such as muscovite, biotite and feldspar. These data suggest that Au itself is one of the best indicators of mineralization in the area.

Primary mineralization at the Federal deposit is indicated by a broad anomaly in the transported overburden. The best sample media appear to be pedogenic carbonates within the soil and hardpanized colluvium at 1-3 m depth. Previous CRC LEME studies in the southern Yilgarn showed good geochemical response in pedogenic carbonates through transported overburden up to 5 and, locally, to 10 m thick (Butt et al., 1997). Chemogenic dispersion through the transported overburden up to 10 m thick at the Federal deposit supports that observations and provides a point for exploration within areas with moderately deep transported overburden. Mechanism of chemogenic Au enrichment within pedogenic carbonates is still unclear and needs further investigation. A detrital source of the calcrete Au anomaly can not be excluded because of variability in sediment cover thickness at the site. Gold could be mechanically transported to the surface in places with thin sediment cover, with further supergene Au mobilization and lateral redistribution in the calcrete environment.

The significance of elevated concentrations of Au in the duricrust colluvium, comprising mostly detrital Au, is unclear. This horizon, which is widely distributed in the area, could probably be of help as sampling media on a sub-regional scale. This can be tested using the database on Au, but it is beyond of the scope of this study.

In the residual regolith, one of possible targets is the top of the saprolite (transition zone) just below BOCO, where minor Au enrichment occurs. Supergene Au enrichment immediately above (up to 20 m) the weathering front is the most pronounced though sampling to this depth (50 m below surface) will involve greater drilling costs. Results indicate that Au dispersion in the saprock follows modern relief (lowering to the east). This feature should be borne in mind for further exploration in the Woodcutters area.

ACKNOWLEDGEMENTS

The authors would like to thank staff of Centaur Mining and Exploration, and particularly Steven Oxenburgh and Stephen Burke for their invaluable assistance and support throughout the research. Dale Longman and Paula Voyd are acknowledged with appreciation for their technical support. Michael Hart is thanked for undertaking XRF analyses and Michael Hart and Dale Longman for XRD analyses. Bruce Robinson and Michael Verrall are acknowledged for assistance with SEM analyses. Angelo Vartesi, Colin Steel and Travis Naughton are thanked for artwork. Annamalai Mahizhnan is appreciated for kindly offered geochemical data on the transported overburden. The authors are grateful to Charles Butt, Matthias Cornelius and Martin Wells for internal review. Charles Butt provided invaluable advice during the preparation of this report.

REFERENCES

- Bristow, A.P.J., Gray, D.J. and Butt, C.R.M., 1996. Geochemical and spatial characteristics of regolith and groundwater around the Golden Delicious Prospect, Western Australia. CSIRO Division of Exploration and Mining Restricted Report 280R, Perth, Australia. 175pp.
- Butt, C.R.M., Gray, D.J., Robertson, I.D.M., Lintern, M.J., Anand, R.R., Britt, A., Bristow, A.P.J., Munday, T.J., Phang, C., Smith, R.E. and Wildman, J.E., 1997. AMIRA P409 – Geochemical exploration in areas of transported overburden, Yilgarn Craton and environs, Western Australia. CSIRO Division of Exploration and Mining Restricted Report 333R, Perth, Australia. 164 pp.
- Churchman, G.J., Whitton, J.S., Claridge, G.G.C., and Theng, B.K.G., 1984. Intercalation method using formamide for differentiating halloysite from kaolinite. *Clays and Clay Minerals*. Vol. 32, No.4. p. 241-248.
- Douglas, G.B., Robertson, I.D.M. and Butt, C.R.M., 1993. Mineralogy and geochemistry of the Lights of Israel Gold Mine, Davyhurst, Western Australia. CSIRO Division of Exploration Geoscience Restricted Report 393R, Perth, Australia. 89pp.
- Drever, J.I., 1982. *The Geochemistry of Natural Waters*. Prentice-Hall, Inc., Englewood Cliffs, N.J. U.S.A. 388 p.
- Freyssinet P. and Butt C.R.M., 1988. Morphology and geochemistry of gold in a lateritic profile, Bardoc Mine, Western Australia. CSIRO Division of Exploration Geoscience Restricted Report MG59R, Perth, Australia. 28pp.
- Gedeon A.Z. and Butt C.R.M., 1990. Morphology and geochemistry of particulate gold in the lateritic regolith, Mystery Zone, Mt Percy, Kalgoorlie, Western Australia. CSIRO Division of Exploration Geoscience Restricted Report 124R, Perth, Australia. 45pp.
- Gray, D.J., 1990. Hydrogeochemistry of the Panglo Gold Deposit. CSIRO Division of Exploration Geoscience Restricted Report 125R, Perth, Australia. 74pp.
- Gray, D.J., 1991. Hydrogeochemistry in the Mount Gibson Gold District. CSIRO Division of Exploration Geoscience Restricted Report 120R, Perth, Australia. 80pp.
- Gray, D.J., 1992a. Hydrogeochemistry of sulphide weathering at Boags Pit, Bottle Creek, Western Australia. CSIRO Division of Exploration Geoscience Restricted Report 237R, Perth, Australia. 13pp.
- Gray, D.J., 1992b. Geochemical and hydrogeochemical investigations of alluvium at Mulgarrie, Western Australia. CSIRO Division of Exploration Geoscience Restricted Report 339R, Perth, Australia. 66pp.
- Gray, D.J., 1993a. Investigation of the hydrogeochemical dispersion of gold and other elements from mineralized zones at the Granny Smith Gold Deposit, Western Australia. CSIRO Division of Exploration Geoscience Restricted Report 383R, Perth, Australia. Vols I and II. 93pp.
- Gray, D.J., 1993b. Investigation of the hydrogeochemical dispersion of gold and other elements in the Wollubar Palaeodrainage, Western Australia. CSIRO Division of Exploration Geoscience Restricted Report 387R, Perth, Australia. Vols I and II. 133pp.
- Gray, D.J., 1994. Investigation of the hydrogeochemical dispersion of gold and other elements at Lawlers, Western Australia. CSIRO Division of Exploration and Mining Restricted Report 26R, Perth, Australia. Vols. I and II. 151 pp.
- Gray, D.J., 1995. Hydrogeochemical dispersion of gold and other elements at Baxter, Western Australia. CSIRO Division of Exploration and Mining Restricted Report 169R, Perth, Australia. 85 pp.
- Gray, D.J., 1996. Hydrogeochemistry in the Yilgarn Craton. CSIRO Division of Exploration and Mining Restricted Report 312R, Perth, Australia. 75pp.
- Keeling J.L., 1993. Microbial influence in the growth of alluvial gold from Watts Gully, South Australia. *Quarterly Geological Notes, The Geological Survey of South Australia*. No.26. p.12 - 19.
- Lawrance L.M. and Griffin B.J., 1994. Crystal features of supergene gold at Hannan South, Western Australia. *Mineral. Deposita*, 29, 391-398.

- Lintern, M.J., and Gray, D.J., 1995a. Progress Statement for the Kalgoorlie Study Area - Steinway Prospect, Western Australia. CSIRO Division of Exploration and Mining Restricted Report 95R, Perth, Australia. 121 pp.
- Lintern, M.J., and Gray, D.J., 1995b. Progress Statement for the Kalgoorlie Study Area - Argo Deposit, Western Australia. CSIRO Division of Exploration and Mining Restricted Report 96R, Perth, Australia. 153 pp.
- Mabbutt, J.A., 1980. Weathering history and landform development. In: C.R.M. Butt and R.E. Smith (Editors), *Conceptual Models in Exploration Geochemistry, Australia*. Journal of Geochemical Exploration, 12: 96-116.
- Mahizhnan A., 2000. Red-brown hardpan in the Federal open pit, Broad Arrow, Eastern Goldfields, Western Australia. CRCLEME Report 133.
- Moore, D.M., and Reynolds, R.C.JR, 1997. X-Ray diffraction and the identification and analysis of clay minerals, Oxford University Press. 378pp.
- Murphy, J. and Riley, J.P., 1962. A modified single solution method for the determination of phosphate in natural waters. *Analytica Chimica Acta*, 27: 31-36.
- Oxenburgh S., 1997. Woodcutters Federal Reserve Report. Centaur Mining and Exploration Ltd Report.
- Parkhurst, D.L., Thorstenson, D.C. and Plummer, L.N., 1980. PHREEQE, a computer program for geochemical calculations. U.S. Geological Survey Water Resources Investigations 80-96, 210p.
- Plummer, L.N., and Parkhurst, D.L., 1990, Application of the Pitzer Equations to the PHREEQE geochemical model, in Melchior, D.C., and Bassett, R.L., eds., *Chemical modeling of aqueous systems II: American Chemical Society Symposium Series 416*, Washington, D.C., American Chemical Society, p. 128-137.
- Porto C.G., Sergeev N.B. and Gray D.J, 1999. Gold distribution, regolith and groundwater characteristics at the Mt Joel prospect, Western Australia. CSIRO Division of Exploration and Mining Restricted Report 553R, Perth, Australia. 95 pp.
- Robertson, I.D.M., Dyson, M., Hudson, E.G., Grabb, J.F., Willing, M.J. and Hart, M.K.W., 1996. A case-hardened, low contamination ring mill for multi-element geochemistry. *Journal of Geochemical Exploration*, 57: 153-158.
- Sergeev N.B. and Gray D.J, 1999. Geochemistry, hydrogeochemistry and mineralogy of regolith, Twin Peaks and Monty Dam gold prospects, Western Australia. CSIRO Division of Exploration and Mining Restricted Report 643R, Perth, Australia. 210 pp.
- Watterson J.R., 1992. Preliminary evidence for the involvement of budding bacteria in the origin of Alaskan placer gold. *Geology*. Vol.20. p.315-318.
- Weast, R.C., Astle, M.J. and Beyer, W.H. (1984). "CRC Handbook of Chemistry and Physics." F-154 Elements in Sea Water. (64th Edition; CRC Press Inc., Florida, USA).
- Witt W.K. and Davy R., 1977. Geology and geochemistry of granitoid rocks in the southwest Eastern Goldfields Province: Geological Survey of Western Australia Report, Vol.49. 137p.
- Zall, D.M., Fisher, D. and Garner, M.D., 1956. Photometric determination of chlorides in water. *Analytical Chemistry*, 28:1665.
- Zhou T. and Phillips N., 1998. The Woodcutters deposit: gold in Archaean granite. Centaur Mining and Exploration Ltd Report.

APPENDICES